

HPLC SEPARATION POST-COLUMN REACTION, UV-VISIBLE
AND FLUORESCENCE DETECTION OF TRACE UO_2^{2+}/U^{4+}
SPECIES IN AQUEOUS SOLUTIONS

By

ABDOL REZA KARIMI

✎

Bachelor of Science
Pars College
Tehran, Iran
1971

Master of Science
Eastern New Mexico University
Portales, New Mexico
1976

Master of Science
The University of Tulsa
Tulsa, Oklahoma
1978

Submitted to the Faculty of the
Graduate College of the
Oklahoma State University
in partial fulfillment of
the requirements for
the Degree of
DOCTOR OF PHILOSOPHY
December, 1986

Thesis
1986D
K18h
Cop. 2



HPLC SEPARATION POST-COLUMN REACTION, UV-VISIBLE
AND FLUORESCENCE DETECTION OF TRACE UO_2^{2+}/U^{4+}
SPECIES IN AQUEOUS SOLUTIONS

Thesis Approved:

Louis P. Varga

Thesis Adviser

E. J. Cisimprum

Horacio A. Mottola

Zuhair al-Hwiti

Norman N. Dunham

Dean of the graduate college

PREFACE

The objective of this study was to use HPLC to separate the U(VI)/U(IV) species in the aqueous samples.

Dr. Louis P. Varga served as major advisor. The others of the advisory committee included Drs. H. M. Mottolla, E. J. Eisenbraun, and Z. Al-Shaib. I am grateful for the guidance of these and many other faculty members and colleagues. Special gratitude is extended to Dr. Horn and Dr. Owens for their kind assistance. I am also thankful to the department of animal science for their assistance and generous help during this study.

A special thanks is given to my wife, Fereshteh, and my sons Ali and Arian, for their patience, understanding, and aid in preparation of this manuscript.

This work is dedicated to the memory of my father who died during the course of this study.

This study was supported by the Oklahoma State University Chemistry Department in the form of Teaching Assistantships.

TABLE OF CONTENTS

Chapter	page
I. INTRODUCTION.	1
History.	1
Analytical Chemistry of Uranium.	4
Oxidation numbers of Uranium.	4
Oxygen Bonding.	5
Nitrogen Binding.	5
Complex Compounds of U(IV).	6
Complex Compounds of U(VI).	6
The State of Uranium Ions in Solution.	7
II. LITERATURE REVIEW	10
Design	11
Introduction.	11
Anion Systems	13
Cation Systems.	14
Chemistry.	32
Introduction.	32
Cation Detection.	32
Absorbance Detection	33
Electrochemical Detection.	35
Fluorescence Detection	37
Spectrometric Detection.	39
Application.	40
Cation.	40
Absorbance	40
Lanthanides	44
Actanides	45
Conclusions.	46
III. EXPERIMENTAL.	47
Direct Fluorometric Measurment of U(VI) in Aqueous Solutions.	47
Reagent and Materials	47
Buffer-Complexing Solution.	48
Uranyl Nitrate Stock Solution	48
Apparatus	48
Limit of Detection and Calibration Curve	50

Chapter	page
Dependence of The Fluorescence Signal on Uranyl Ion Concentration and Amount of Buffer Solution Added	53
Interferences by Cations.	56
Interferences by Anions	62
HPLC Separation Post-Column Fluorometric Determination of U(VI) in Aqueous Solutions.	62
Reagents and Materials.	65
Apparatus	65
Chromatographic Parameters.	67
Optimization of The Reaction Coil	69
Calibration and Detection Limit	71
Interferences	71
HPLC Separation and PCR Detection of U(VI) And U(IV) Ions in aqueous solutions.	71
Reagents and Materials.	74
Apparatus	74
Synthesis of Ligand	75
Uranium(VI)/(IV) Stock Solutions.	76
Mobile phase And PCR Solutions.	77
Procedure	77
Chromatographic Parameters.	78
Effect of pH and Ionic Strength of the buffer solution on U(IV)/U(VI) Separation.	80
Effect of Alkylsulfonates Chain length on k' Value.	82
Calibration Curve and Detection Limit	82
Interferences	87
IV. RESULTS AND DISCUSSION.	88
Direct Fluorometric Determination of U(VI) in Aqueous Solutions.	88
HPLC Separation Post-Column Fluorometric Determination of U(VI) in Aqueous Solutions	92
HPLC Separation and PCR Detection of U(IV) and U(VI) Ions in Aqueous Solutions	94
V. SUMMARY	98
BIBLIOGRAPHY	101

LIST OF TABLES

Table	page
I. Effect of Ionic Strength of Solution on Hydrolysis of Uranyl Ion.	9
II. PCR Band Broadening.	21
III. Chromatographic Parameters For U(VI) Separation on Cation-Exchange Column.	69
IV. Chromatographic Parameters For U(IV)/U(VI) Separation on C ₁₈ Column	80

LIST OF FIGURES

Figure	page
1. Cross Section of Zero Dead-Volume Cell Used to Mix Eluate and Post-Column Reagent	16
2. Schematic of a Mixing T	18
3. Schematic of Reagent Addition Through a Hollow Fiber	20
4. Schematic of Improved Mixing T	28
5. Mixing Pattern of Benzene and Methanol With Different Mixing Designs	29
6. HPLC Analysis of Uranium.	34
7. HPLC Analysis of Uranium With 0.3 mol/liter Carbonate in Post-Column Reagent Solution	35
8. Optical Diagram of Spectrofluorometer	49
9. Excitation and Emission Spectra of an Aqueous Solution of $\text{UO}_2(\text{NO}_3)_2 \cdot 6\text{H}_2\text{O}$	51
10. Calibration Curve for Uranyl Nitrate Solution	52
11. Minimum Detectable Amount of UO_2^{2+} , Using Signal-to-Noise Ratio Method.	54
12. Fluorescence Intensity of Uranyl ion in Phosphate Buffer As a Function of Buffer Content	55
13. Fluorescence Intensity of Uranyl Ion in 30 ml Phosphate Buffer As a Function of Uranium Content	57
14. Fluorescence Intensity of Uranyl Ion in Phosphate Buffer As a Function of Na^+ , K^+ , and Mg^{2+} Concentrations	58

Figure	page
15. Fluorescence Intensity of Uranyl Ion in Phosphate Buffer as a Function of Mn(II) Concentration	59
16. Fluorescence Intensity of Uranyl Ion in Phosphate Buffer as a Function of Fe(III) Concentration	60
17. Fluorescence Intensity of Uranyl Ion in Phosphate Buffer as a Function of Ca(II) Concentration.	61
18. Fluorescence Intensity of Uranyl Ion in Phosphate Buffer as a Function of NO_3^- , SO_4^{2-} , and CO_3^{2-} Concentrations.	63
19. Fluorescence Intensity of Uranyl Ion in Phosphate Buffer as a Function of Cl^- Concentration.	64
20. Schematic of Micro-Mixer Manufactured by LEE Company	66
21. Post Column Reaction System Components.	68
22. Chromatogram of Uranyl Nitrate Injected on Cation-Exchange Column.	70
23. Optimization of Reaction of Reaction Coil Length.	72
24. Calibration Curve for Uranyl Nitrate Solution.	73
25. Chromatogram of U(IV)/U(VI)	79
26. Dependence of the Capacity Factor of U(VI) and U(IV) on the Acetate Buffer Concentration	81
27. Dependence of the Capacity Factor of U(IV)/U(IV) on the Chain Length of the Alkylsulfonates	83
28. Dependence of the Capacity Factor of U(IV)/U(VI) on the Concentration of Hexanesulfonate	84
29. Calibration Curve for U(IV) on C_{18} Column	85
30. Calibration Curve for U(VI) on a C_{18} Column	86

CHAPTER I

INTRODUCTION

History

The element uranium was discovered in 1789 in the pitchblende ores of Saxony by M.H. Klaporth (1743-1817).

The Discovery of uranium was the final step in attempts that had been going on for a long time to classify the mineral pitchblende, found in Joachimsthal (Bohemia) and also in Johangeogenstadt (Saxony) [1]. On treating pitchblende with nitric acid, Klaporth obtained a yellow solution, from which a yellow precipitate could be isolated when "potash" was added. He considered this precipitate to be the oxide of the new element and indeed secured a substance which had a metallic appearance when it was heated with carbon at a high temperature. Klaporth believed this to be the metal itself, but we know that was in fact a uranium oxide.

Klaporth described his discovery on the 24th of September 1789, in a lecture given before the Royal Prussian Academy of Science [2], when he named the new element "uranit", after the planet uranus, discovered some years

before (1781). A year later Klaproth changed the name to uranium.

By 1789, Klaproth had already isolated the nitrate, sulfate, acetate and formate of uranium as well as potassium and sodium uranates. In many publications he described the preparation and properties of these compounds, but until his death in 1817 he remained convinced that he had isolated the element.

Berzelius, who studied the material "uranit" soon after its discovery, suspected that it was not the element, but was unable to reduce it further by the use of potassium. It was more than half a century after Klaproth's discovery that the French chemist E.M. Peligot proved with certainty that "uranit" was not the element itself, but an oxide. This he did by passing chloride over a heated mixture of "uranit" and carbon and so produced besides uranium chloride, a mixture of CO and CO₂. Peligot was also the first to prepare the metal. In 1841, he heated anhydrous uranium tetrachloride with potassium in a platinum crucible. After the product had been cooled potassium chloride was leached out with water. The black residue contained pieces of uranium with silvery luster. The density of the metal was not determined.

Later in 1856, Peligot prepared a pure product by melting UCl₄ with sodium in porcelain in the absence of air, the density of this metal was 18.4 which is reasonably close to the value 19.05 now accepted for the pure metal. He also

described some of the more important properties of uranium; for instance its rapid oxidation at higher temperatures. He also determined its atomic weight, for which he found the value 120. However, D.I. Mendeleev in 1869 was unable to accept this since it brought uranium between silver (108) and iodine (127) in his periodic table. This place was not in accordance with its properties and he, therefore, doubled the value. As a result, he obtained a good periodicity in the properties of uranium and the analogous elements tungsten, molybdenum and chromium.

Indeed several investigations into the properties of uranium were studied in the years following. In particular those by C.Zimmermann confirmed that the atomic weight of uranium had been correctly identified to be 240.

Determination of the vapor density of UCl_4 and UBr_4 , according to the method of V. Meyer, yielded the value 242.2. At that time interest in the properties of the element was purely academic. Uranium compounds were of little economic importance and used only on a very small scale, mainly for coloring glass and porcelain. Uranium metal itself was tried at the end of the 19th century as a substitute for tungsten in tools for war applications. But none of these applications involved quantities of any importance and the deposits of uranium ores at Joachimsthal (Austria) were mined mainly to satisfy the demand for thorium.

This was the position until the discovery of radioactivity by Bacquerel (1896) and later that of the presence of radium in uranium ores (1898). When the demand for uranium suddenly increased, the deposits of uranium ores at Joachimsthal and those in the Belgian Congo and in Canada were mined for their radium content. However, until 1942 no mining operations were carried out for uranium production.

The advent of the nuclear age, brought about by the almost simultaneous discovery of nuclear fission (1938/39) and the outbreak of the second World War, a new interest in the element uranium and its compounds; such interest has grown rapidly since that time.

During and after the second World War, much new information on the chemistry of uranium had been gathered in the United States as part of the Manhattan Project. It was only after the first "Conference on the peaceful uses of atomic energy", held in Geneva in 1955, that much of this knowledge became available.

Analytical Chemistry Of Uranium

Oxidation Numbers of Uranium

The chemical properties of uranium are characterized to a considerable extent by the closeness of its electronic energy levels, the mutual distribution of which varies somewhat under the influence of various factors and, in particular, depends on the element combined with it to form

compounds. The oxidation numbers of uranium in its compounds vary from +2 to +6, but the typical values are +4 and +6, the later being the more stable one in the presence of atmospheric oxygen.

The formal potential of the system U(VI)/U(IV) in a 1 M solution of HClO_4 at 25 C^0 has been found to be +0.334 volts [3], making U(IV) the stable state in the absence of oxidizing agents. Separation procedures including extraction, ion-exchange and precipitation make use of these two oxidation states U(VI) and U(IV) to selectively separate uranium from interfering ions in natural waters.

Oxygen Bonding

Although stability constants for some uranium complexes and chelates involving oxygen bonding are not high, sufficient stability exists for their use in separation and spectrophotometric methods. Extraction and spectrophotometric determination of uranium (VI) based on tributylphosphine oxide and 8-hydroxyquinoline are examples of oxygen coordination to uranium [4].

Nitrogen Bonding

The stability of the uranyl-nitrogen bond is low. Thus EDTA and similar nitrogen coordinating complexing agents are effective for masking interfering ions in U(VI) determinations. Nitrogen bonding of U(IV) with azo compounds such as arsenazo and the azide ions is

sufficiently stable to be useful for the spectrophotometric determination of U(IV) after separation [5].

Complex Compounds of U(IV), The Aqueous U^{4+} Ion

The ion U^{4+} is a complex-forming ion with a large radius ($r = 1.05 \text{ \AA}$); in this respect it comes close to Th^{4+} , and Zr^{4+} . The systematic investigation of the properties of some anionic complexes of U^{4+} (sulfate, carbonate and oxalate) show that the coordination number of U^{4+} is eight in the majority of the cases.

Tetravalent uranium also forms complexes with oxalate, fluoride and carbonate. The instability constant of these complexes have been studied [6]. The U^{4+} ion forms complexes with numerous organic compounds [7]. Complex compounds of U^{4+} with hydroxy acids (tartaric, citric, etc) amino acids and diketones have been described [8].

Complex Compounds of U(VI), The Aqueous Uranyl Ion UO_2^{2+}

There have been many investigations of uranyl complexes [9], and it has been established that UO_2^{2+} can form both anions and cations complexes. Data obtained by the study of electrophoresis of aqueous uranyl solutions are of interest [10].

Uranyl ions form numerous complexes with $SO_4^{=}$, NO_3^- , Cl^- , $CO_3^{=}$, etc. ions. Their compositions are established by physiochemical investigation of the solid state and of their aqueous solutions.

Most of the complexes of uranyl ion with inorganic compounds are colorless and readily soluble in water. Their existence should be taken into account in the separation of uranium by extraction as well as in its determination by various methods.

In the chemistry of uranyl ion, its complexes with organic reagents are of great importance. Uranyl ions forms soluble complexes with a wide variety of complexing ligands found in water. These may include complexes with organic ligands derived from components of humic acids and other organic matter.

Citric, tartaric, malic and lactic acids form uranyl complexes which are stable even at high value of pH (8 to 10). Ethylenediaminetetraacetic acid (EDTA) and its disodium salt form weak complexes with the uranyl ion. This makes it possible to use EDTA in the analytical chemistry of uranium as a masking agent in the separation and determination of the uranyl ion [11].

Chelates of the uranyl ion with 8-hydroxyquinoline and its derivatives have been described, as well as those with derivatives of azomethane, and many other organic ligands, such as arsenazo I, II and III [12,13].

The State of Uranium Ions in Solution

Uranium(IV) is present in acid aqueous solutions as the simple hydrated ion, $U(H_2O)_n^{4+}$ where $n = 6$ or 8 . Solutions

of U(IV) salts are acidic, which indicates hydrolysis. The hydrolysis is known to proceed according to the reaction:



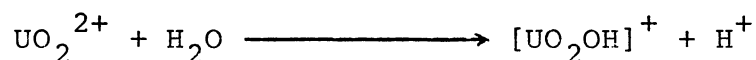
When the hydrolysis is extensive, polynuclear ions of the type $\text{U}[(\text{OH})_3\text{U}]_n^{4+n}$ and also polymers $[\text{U}(\text{OH})_4]_x$ may be formed.

Cold acid solutions of U(IV) are fairly stable in the dark. It has been shown that the oxidation of U(IV) in air is appreciably accelerated by light, especially by direct sunlight and ultraviolet light.

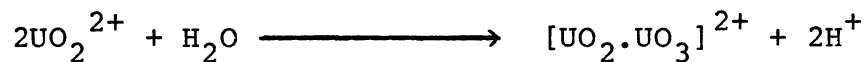
Uranium(VI) is present in solutions as the hydrated ion UO_2^{2+} the existence of which at $\text{pH} < 2.5$ has been firmly established [14]. At higher pH values composite hydrolyzed ions such as $[\text{U}_3\text{O}_8(\text{OH})]^+$, $\text{U}_3\text{O}_8(\text{OH})_2$, $[\text{U}_3\text{O}_8(\text{OH})_3]^-$, $\text{U}_2\text{O}_5^{2+}$, $\text{UO}_2(\text{OH})^+$ etc. predominate.

Many investigations indicate the incomplete dissociation of uranyl salts in aqueous solutions [15]. For instance, it has been found that in concentrated nitric acid solution uranium is present chiefly as undissociated molecules of $\text{UO}_2(\text{NO}_3)_2$. Data on electrical conductivity of aqueous solutions of uranyl sulfate indicate the incomplete dissociation of UO_2SO_4 [16].

The hydrolysis of UO_2^{2+} can be explained by the formation of the monomer $[\text{UO}_2\text{OH}]^+$ in the reaction:



and of the dimer $[\text{UO}_2 \cdot \text{UO}_3]^{2+}$ which is formed in the reaction;



The relationship between equilibrium constants K_1 and K_2 for the two reactions above, and the ionic strength of the solution is shown in Table I [17].

TABLE I
EFFECT OF IONIC STRENGTH OF SOLUTION ON
HYDROLYSIS OF URANYL ION [ref. 17].

Condition (ionic strength, μ , and temperature $^{\circ}\text{C}$)	K_1	K_2
$\mu = 0.347$; 25	4×10^6	1.5×10^6
$\mu = 0.0347$; 25	1.5×10^6	0.7×10^6
$\mu = 0.0347$; 45	8×10^6	1.2×10^6

CHAPTER II

LITERATURE REVIEW

Present methods available for the determination of U(VI) in aqueous solutions are often tedious and time consuming, especially at very low concentrations (e.g. ng/ml). Such trace determinations are of particular importance to the uranium mining industry and to nuclear waste-management studies. Recently, it has been shown that high-performance liquid chromatography (HPLC) with post-column reaction (PCR) offers considerable potential for the determination of trace quantities of metal ions [18-21].

Unlike the development of chromatographic technique for the determination of organic species, the progress of modern inorganic liquid chromatography (LC) has been very dependent on the application of PCR systems, and PCR detection still remain the dominant detection technique for inorganic species in general. This is changing slightly as new chromatographic techniques are developed that permit the direct detection of eluted species, but it is certain that PCR system will continue to play an important role in the development of inorganic liquid chromatography. This review will attempt to cover the important developments that have

been taken place in the separation and detection of inorganic species, especially actinide and lanthanide ions by HPLC and PCR since Lundgren and Loeb [22] reported the first inorganic LC-PCR system for the separation of inorganic phosphates.

With the exception of the work of Takata and that of Fritz [23,24], which are discussed elsewhere in this review, very little has been reported on inorganic LC until 1975. In 1975, the future of inorganic LC changed dramatically with the introduction of suppressed ion chromatography by Small, et al. [25]. This system was essentially a PCR that removed the background salts from the eluent used for the ion-exchange separation of inorganic ions and thus permitted sensitive conductometric detection. This principle was eventually marketed by the Dionex Corporation, primarily for the separation of inorganic anions, and the PCR used was a packed-bed ion-exchange resin that exchanges hydrogen ions for eluent cations.

This review has been divided into three main sections: design, chemistry, and applications, each of which is divided into a discussion of anions and cations.

Design

Introduction

Although the first application of a PCR for the detection of inorganic species eluted from a chromatographic column took place in 1961 [22], there have been only

a few studies published on the effect of different design factors on the performance of the PCR for inorganic species. Fortunately, most of the design features developed for the detection of organic species can be applied to the detection of inorganics. Many of the PCR systems developed for organic analysis are useful where PCR chemistry is complex, and this is the case for most of the reported anion PCR systems. However, in the majority of the inorganic PCR systems published to date, the PCR chemistry has been fast and relatively simple. Consequently, reactor beds and /or delay coils, between the point of reagent addition and the detector, are often not required, and this can reduce concerns about band broadening for analytes with low K' (capacity factor) values. To eliminate extra-column band broadening, the mixing of the reagent and eluate must take place in a very small volume, $<2 \mu\text{l}$ for modern columns packed with 3- and 5- μm particles. The mixer design and the techniques used for reagent addition can have important effects on detection, effects that are usually not a concern for more complex organic PCR systems. It has been only in the last 3-4 years that people have begun to adequately address this aspect of inorganic PCR detection.

The following section discusses the results published on the design of inorganic PCR systems. Some of the papers have been included for historical reasons, but for the most part emphasis has been placed on papers that discuss design features that affect performance of the PCR-HPLC system. A

summary of some important design aspects is given at the end of this section.

Anion Systems

The autoanalyzer principles of the Technicon system were used in a number of the early applications of PCR systems [22,26] to LC. It is interesting to note that these first systems involved the development of rather complex PCR chemistry and worked remarkably well considering the stage of development of LC at that time. In 1961, Lundgren and Loeb [22] reported the first application of continuous flow PCR detection for the LC determination of condensed phosphate ions after separation on ion-exchange columns; this system was modeled after the pioneering work of Spackman et al. [27], who developed an automated ion-exchange procedure for the determination of amino acids. In this work the eluted phosphate species were introduced into a Technicon autoanalyzer from an ion-exchange bed containing 100-200 mesh AG1-X8 anion resin and detection was based on the measurement of phosphorus by the molybdenum blue method. Because the resolution of this column was poor, at least by present-day standards, band broadening and mixing efficiency were not a concern and were not investigated; this has also been the situation for most of the more recent studies involving the application of autoanalyzers to PCR detection of inorganic species.

In 1978, the application of PCR detection to the separation of condensed phosphates was reinvestigated by Deelder et al. [28]. These workers developed an air-segmented PCR system, similar in chemistry to that described by Lundgren and Loeb [22]. However, the cross-linked resin used had a smaller particle size, and the PCR components were miniaturized, thus reducing the band broadening associated with the reaction system.

Hirai et al. [29,30], who have also applied an autoanalyzer-based PCR to the LC separation of polyphosphates developed a FIA system that was more compatible with modern high-resolution columns than the autoanalyzer. Band broadening was less with the FIA-PCR, and this was illustrated by increased sensitivity and improved resolution; calculations from the data reported in their paper show that the value for HETP (height equivalent to a theoretical plate) had improved to about 0.6 mm from the 1-2 mm value obtained previously when this column was interfaced to a Technicon-based system [31].

Cation Systems

The early studies on the application of PCR systems to the detection of metal ions were limited to low-resolution columns, and the mixers used for reagent addition had appreciable dead volumes; however, some of these studies, notably those of Fritz et al., which are discussed below, formed the basis of future applications to high-resolution

systems. Most of these detection systems were based on the measurement of absorbance after the addition of colorimetric reagents, and this is still the most commonly used technique in the majority of the reported application of PCR systems for the detection of metal ions.

In 1971, the first thorough study of the LC determination of metal ions with continuous detection was reported in a thesis by Sickafoose [32], who was working under the direction of Fritz. This study included the investigation of different designs of mixing devices, and a divided tangential-entry whirlpool design was effective for the low-resolution columns used. This type of mixer was used by Fritz in some of his subsequent studies on metal ion separations and column development. Other design features reported in the early development of metal PCR detection included the use of hollow tubes as mixers [33,34], the application of Technicon technology [35], and the use of a small turbo-mixer (100 μ l) in which the mixer blade was driven by the laboratory air supply (34). Although these mixers worked well for these studies, the large volume of mixers would be a limitation for applications to modern high-performance columns.

In 1979, Elchuck and Cassidy [36] reported the first application of PCR detection to the high-resolution separation of metal ions using 5- and 10- μ m bonded phase exchangers and a 13- μ m resin. The detection systems developed were based on reagents used in the earlier work by

Story and Fritz [37]. Several designs of low dead-volume (1-10 μ l) mixers were investigated, and the best design was a modified T which is shown in Figure 1.

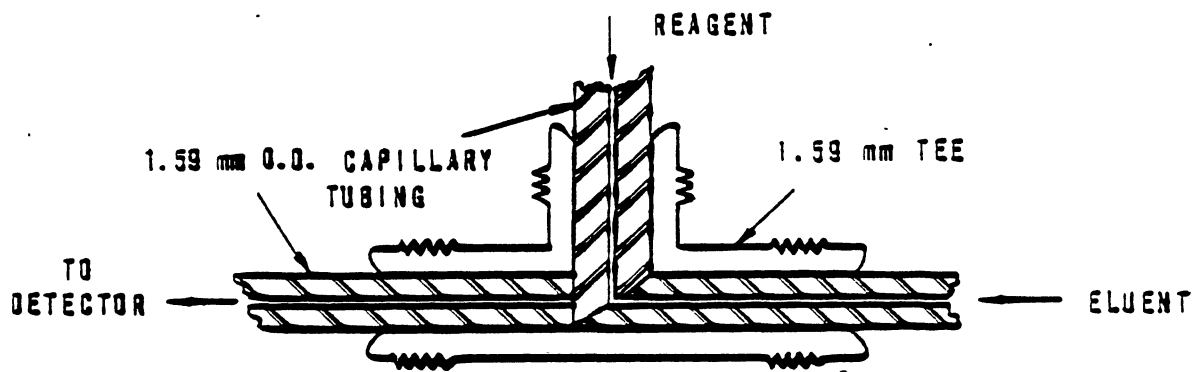


Figure 1. Cross section of zero dead-volume cell used to mix eluate and post-column reagent. All tubing is 0.15-mm ID. [ref. 36]

The two inlet tubes were cut at 45° and butted up against one another; the mixed eluate and reagent flowed out and around the small spaces between the tubes and then into the exit tube to the detector. The holdup time between the end of the column and the detector was about 1-msec, and the total dead volume was less than 3 μ l. The reactions between the metal ions and the reagents used [4-(2-pyridylaso)-resorcinol, PAR, and Arsenazo-I] were essentially complete in this time span as the sensitivities obtained were in reasonable agreement with those calculated from measured values of molar absorptivities. The total variance σ^2 for the mixer, detector and injector was 0.03 sec^2 with a flow rate of 1 ml/min for both the eluent and reagent.

The factors determining the magnitude of the baseline noise were investigated, and it was found that the two most important parameters were mixing efficiency and background absorbance. The effect of the first of these parameters was minimized by optimization of the design of the mixer (Fig. 1) and by reducing pressure pulsations from the pump with pulse-dampening devices. Noise arising from pressure fluctuations was also minimized by the use of a constant-flow screw-driven syringe pump to introduce the reagent solution. The background absorbance was minimized by keeping the concentration of the post-column reagent as low as possible without limiting its ability to react with the metal ion over a reasonably wide concentration range: the optimum reagent concentration was found to be 2×10^{-4} mol/liter for Arsenazo-I. This concentration gave a linear working range of 10-600 ng. Because background absorbance from the reagent was directly or indirectly the main source of noise in this detection system, the signal-to-noise ratio was not maximized at the wavelength of maximum absorbance for the metal complex; the maximum signal-to-noise ratio was obtained at the wavelength where the ratio of the absorptivities of complex to reagent was maximized. For PAR and Arsenazo-I, these maxima were at 540 nm (λ_{\max} is 490 for PAR complexes) and at 600 nm (λ_{\max} is 585 nm for Arsenazo-I complexes), respectively. Background absorbance for PAR was further minimized by keeping the pH of the reactant solution at 9.7; this suppressed the acid

dissociation of PAR, which enhanced reagent absorbance at these wavelengths. The peak-to-peak noise was maintained at 5×10^{-4} absorbance units with a reagent solution having an absorbance of 0.07 units versus the eluent. The amount of metal ion required to give a response equivalent to twice the peak-to-peak baseline noise for PAR and Arsenazo-I was 0.1 and 1.0 ng, respectively, for most of the lanthanides studied.

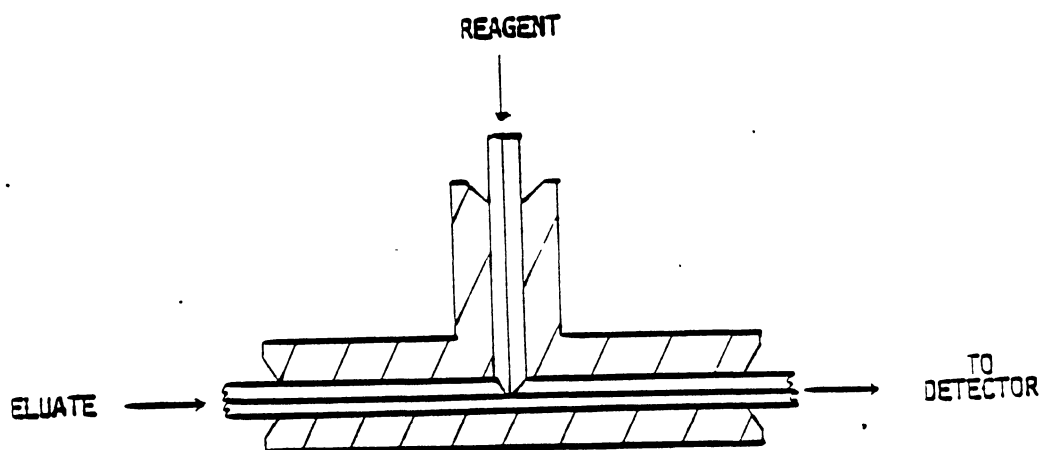


Figure 2. Mixing T: 1/16-in. OD X 0.007-in. ID tubing in a boredout T. [ref.38].

In 1984, Schmidt and Scott [38] described a PCR system that was based on that reported by Elckuk and Cassidy [36]. The mixer design was somewhat different and is shown in Figure 2. It was constructed out of 1/16-in. OD X 0.007-in. ID stainless steel tubing, and an 8-cm length of the tubing was radially bored in the center (with a 60° cut) to intersect the inner conduit. The reagent inlet tube was cut to fit into this hole, and the two tubes were held in place

with a drilled out T. The contribution to dispersion from this mixer was determined to be the same as that for a straight length (8 cm) of the 0.007-in. ID tubing. The performance of this mixer was illustrated, but, as the absorbance scale used was not given, the magnitude of the peak-to-peak noise can not be determined. The residual mixing noise was eliminated by incorporating a 5 cm length of low dispersion tubing. The construction and operation of this type of tubing has been described [39], and the contribution to band broadening by this form of mixer appears to be minimal for most HPLC applications.

The first commercially available PCR designed for the detection of metal ions (Dionex) was based on the absorbance of visible light by metal chelates and resembled that described by Elchuk and Cassidy [36] and Story and Fritz [37]. The operation of this PCR has been described briefly in a technical memorandum [40] by Riviello. The eluent and reagent (PAR) were mixed via a T and then introduced into a packed-bed reaction coil. Detection limits were in the high picogram to low nanogram range, but the reaction coil gave noticeable band broadening [41] and the baseline noise was 6×10^{-4} absorbance units. Recently, Dionex has introduced a unique type of a PCR system where the reagent addition occurs via effusion through a semipermeable membrane [41]. A schematic of this PCR is shown in Figure 3. The eluent flowed into a semipermeable hollow fiber, the outside of which was exposed to the PCR reagent solution.

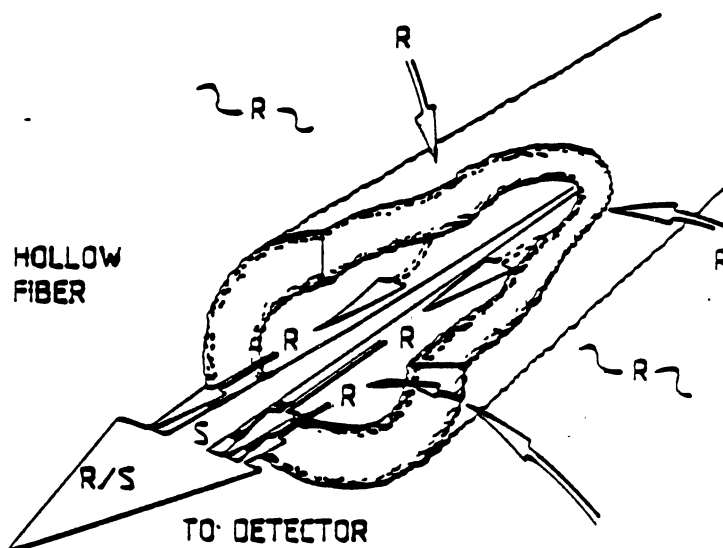


Figure 3. Schematic of reagent addition through a hollow fiber. Typical fiber length is 380 mm, and the diameter is 0.5 mm, [ref. 41].

This reagent solution was placed under pneumatic pressure and thus passed through the hollow fiber into eluent. The membrane reactor was made of inert materials which minimized reagent contamination, and was compatible with acids, bases, methanol, ethanol, and propanol, but not with other organic solvents. Some comparisons were made between this PCR and conventional PCR detection, but unfortunately the condition used for this comparison are not given. The authors claim improved radial mixing relative to other PCR devices, due to the perpendicular addition of the reagent to the eluent flow, and decreased longitudinal mixing; however, it is not clear why this should be so when one considers that the mixing T's described above introduce the two solutions at

90⁰ to each other and have very small dead volumes. The flow rate

TABLE II
PCR BAND BROADENING

PCR type	Hight equivalent to theoritical plate [*]					
	Pb	Cu	Cd	Co	Zn	Ni
Membrane (100 ul)	0.27	0.067	0.074	0.044	0.050	0.068
Packed tube (170 ul)	0.30	0.092	0.072	0.050	0.050	0.071
Open tube (800 ul)	0.41	0.23	0.25	0.070	0.070	0.079

*The retention times from Pb to Ni were 2, 3, 4, 5, 10, and 13 min, respectively. [ref 39].

affected column efficiency and peak symmetry, and both decreased with increased flow rate.

A comparison between peak asymmetry and column efficiency was obtained at an eluent-flow of 0.5 ml/min. The dead volume of this reactor is appreciable (100 μ l) and can contribute to band broadening, as shown by the data given in Table II. The data shown in Table II indicate that band broadening may occur for peaks with retention below 3-7 min; with a 10 μ m packing, such as that used to obtain the data in Table 2, one would expect HETP values of about 0.05-0.06 mm. The data also show that band broadening is similar for the packed tube and the membrane. Some features of this membrane PCR, such as the use of pneumatic pressure to introduce the reagent, and the dampening of pump pulsations

by the flexible hollow fiber tubing may help reduce background noise. The authors claim a fivefold improvement relative to their conventional PCR, and with this improvement the peak-to peak baseline noise was about 1×10^{-4} absorbance units. Similar noise levels were also given in Dionex product bulletin LPN 32327 10/1983. The detection limits reported were very good (high picogram to low nanogram range) and were about the same magnitude or slightly better than those reported for a T type of mixer [42]. The annular membrane suppressor described by Dasgupa [43], which has solid filament inside the hollow fiber, may reduce the band-broadening effects of the Dionex membrane reactor but has not yet been applied to the detection of metal ions.

In 1981, Hirose et al. [44] reported the first application of microcolumn LC and PCR for the separation and detection of metal ions. The authors had previously separated the rare earths on microcolumns but had used fraction collection and radiochemical measurements to determine the elution profile. In this paper a colorimetric reagent, xylenol orange, was used for the PCR detection of the rare earths. The metal ions were separated on a 6- μ m cation-exchange resin packed in a 0.5-mm ID PTFE tube, and this column was connected to a stainless steel T of 0.33-mm ID. This T was also connected to the reagent solution and to a stainless steel reaction coil (0.19-mm ID X 520 mm). The absorbance cell was made out of PTFE tubing (0.3-mm ID)

and was placed on a slit of 0.18-mm width and 2-mm length. Although the separation was not as good as that obtained with more conventional HPLC systems, it was quite remarkable when one considers that the baseline separation required only 450 μ l of mobile phase. The amount of each rare earth injected was in the range of 0.3-0.8 μ g, and calibration curves were linear up to absorbances of 0.9. The efficiency of mixing and the magnitude of baseline noise were not discussed.

The majority of the PCR designs discussed above were designed for detection systems based on the formation of metal chelates. Recently, two PCR systems have been reported that are based on the destruction of metal chelates [45,47]. Marsh et al. [45] have described a PCR for Pt(II) complexes that was based on a reaction between the complexes and bisulfite in the presence of dichromate. The PCR required a considerable time delay because of the complex chemistry of the reactions. An air-segmented PCR was initially examined, but the surfactant properties of the mobile phase prevented the complete removal of the air bubbles. The use of packed-bed reactors was also examined, but they generated excessive backpressure and band broadening. The authors finally chose the braided Teflon tube (0.3-mm ID) design by Englehardt and Neue [46] and found no significant band broadening after the insertion of 47.8 m of the braided tube. This is quite impressive when

one considers that the column used was a high-efficiency 5- μm C_{18} reversed phase.

The second paper that described a detection system that depended on the destruction of metal chelates was published by Shih and Carr [47]. The authors' previous experience in the application of dithiocarbamate chelating agents for the HPLC separation and determination of metal ions as metal chelates led them to the development of a unique photochemical reactor for the fluorescent detection of metal ions; the aim of this work was to improve the sensitivity of this mode of HPLC for the determination of metals relative to that obtained with direct UV or electrochemical detection. The photochemical reactor consisted of a 10-m length of a 0.25-mm ID Teflon tube coiled (6-cm diameter) around a medium-pressure 175-W mercury lamp. The contribution to band broadening was determined to have little effect on the column resolution for the n-butyl-2-naphthylmethyl-dithiocarbamate metal chelates, but the 90-cm, 10- μm C_{18} column gave a relatively low column efficiency of approximately 3000 plates, or a HETP of 0.3 mm. The value of σ_v for the reactor was 42 μl , and this could be significant if 5- μm packings with HETP values of 0.03 mm are used. The authors have pointed out that a reactor fashioned out of knit coils of tubing [48] could provide less peak dispersion.

Extraction systems have not been applied to the detection of metal ions but would conceivably be very useful

for PCR detection based on the formation and extraction of water-insoluble chelates. The addition of organic solvents to the eluate to increase the solubility of metal chelates has been used [49], but this leads to precipitation of salts that are in the eluent, to an increase in baseline noise due to heat of mixing, and to poorer mixing in general.

Lawrence et al. [50] have described an extraction system that was designed for the detection of organics, but the principles involved in this ion-pair extraction system should be applicable to the detection of inorganics. Solvent segmentation was used to efficiently extract a fluorescent ion pair into an organic phase, and the segmentation of the eluent limited band broadening to 2 s for a 1.4-min extraction time in a 2 mm ID tube operated at a flow-rate of 1 ml/min. The conventional Technicon phase separator was the dominant factor affecting band broadening (12 sec. total), and redesign of this unit could reduce these band-broadening effects. Apffel et al. [51] have also described an extraction system for miniaturized LC that should help eliminate band-broadening effects.

The main function of a PCR system is to promote a reaction with eluates of interest or reproducibly produce new chemical species that were not present during the chromatographic process but that can be directly related to the concentration of the eluates. For most inorganic applications this goal is relatively easy to achieve. However, the maximization of detector sensitivity is not an

easy task, and detector noise produced by the PCR can seriously reduce the detection limits that are theoretically possible. The detection limits for a typical PCR employing absorbance detection depend on the following factors;

1. Sensitivity of the analytical signal
2. Detector noise
3. Background signal
4. Mixer efficiency
5. Pump pulsations

The sensitivity is dictated by the chemistry chosen for PCR detection. For the detection of metal ions with a colorimetric reagent, the absorptivity of the metal complex establishes the slope of the analytical response curve, and it is this slope that determines the sensitivity. Noise from the detector itself is not normally of concern, since 3, 4 and 5 above are usually more important; however, temperature changes can have important effects and must be considered where heating is used or where heats of mixing are large.

As for any analytical technique, the background signal must be minimized to reduce detector noise. For PCR detection, however, a more important factor is the magnitude of the difference between the background signals for the reagent solution and the eluate. This difference will determine the magnitude of the baseline noise arising from poor mixing in the PCR and from pump pulsations, both of which are discussed below. For most analytical techniques, experimental conditions are adjusted to maximize the

analytical response; for absorbance detection, this corresponds to selection of a wavelength that corresponds to the maximum absorbance of the analyte. To improve PCR detection limits, however, it is the signal-to-noise (S/N) ratio that must be maximized, and the maximum S/N is not always located at the point of maximum analytical response. Often a small sacrifice in the analytical response can be traded for a significant decrease in background signal and thus an increase in S/N. Because the reagent used can be a major source of the background signal, efforts must be made to minimize this absorbance by controlling reagent concentration, eluent and reagent purity, and such experimental parameters as pH, which can affect reagent absorbance.

When reagents are added to the eluate in PCR detection, the mixing must be efficient or excessive baseline noise will be obtained. For detectors based on absorbance measurement the magnitude of the baseline noise produced for a given precision of mixing is directly dependent on the difference in absorbance between the reagent and the eluate. Many workers have used mixing coils or packed-bed mixers to ensure homogeneous mixing, but this approach will introduce some additional band broadening, especially for early peaks, and should not normally be used. Packed-bed reactors can be used for slow reactions, but these are designed to give negligible mixing. Attempts have been made to make efficient mixers that contain some dead volume that can be

used for the mixing process. Some of these, such as the divide-entry tangential whirlpool mixer[32], work quite well for medium-resolution columns, but the dead volume of such devices should ideally be kept at $\sim 2 \mu\text{l}$ or less for modern columns. Many workers have used modified Ts for both reagent addition and mixing, and two of these were described earlier in this section. Another design that is quite efficient and very simple to construct is shown in Figure 4.

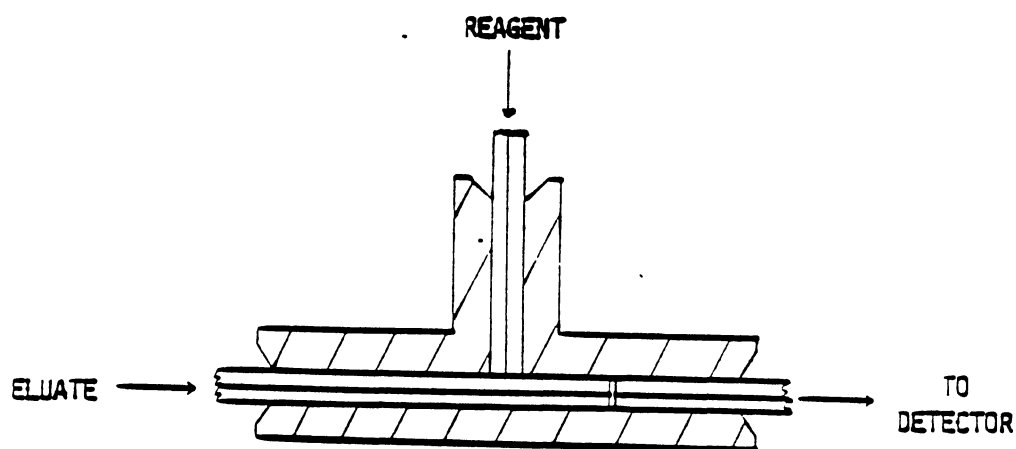


Figure 4. Schematic of improved mixing T. All tubing is 1/16-in OD and a 120-mesh stainless steel screen is positioned between eluate inlet and detector outlet tubes. (ref. 32)

All the tubing is cut square and is held in place with finger-tight plastic fittings; the position of the 120-mesh screen is not important as long as it is placed away from the reagent inlet. The reagent solution flows between the walls of the tubing and the T and then into the screen. This mixer has very little dead volume and gives very efficient mixing over the range of flow rate normally used ($> 0.5 \text{ ml/min}$); some increased noise is observed at lower flow rates, and this could be of concern for applications to

microbore columns. The mixing inhomogeneity from these devices is $<0.08\%$, and further design improvements would be of limited use until the large contribution to noise from pump pulsations is eliminated short-term changes in flow

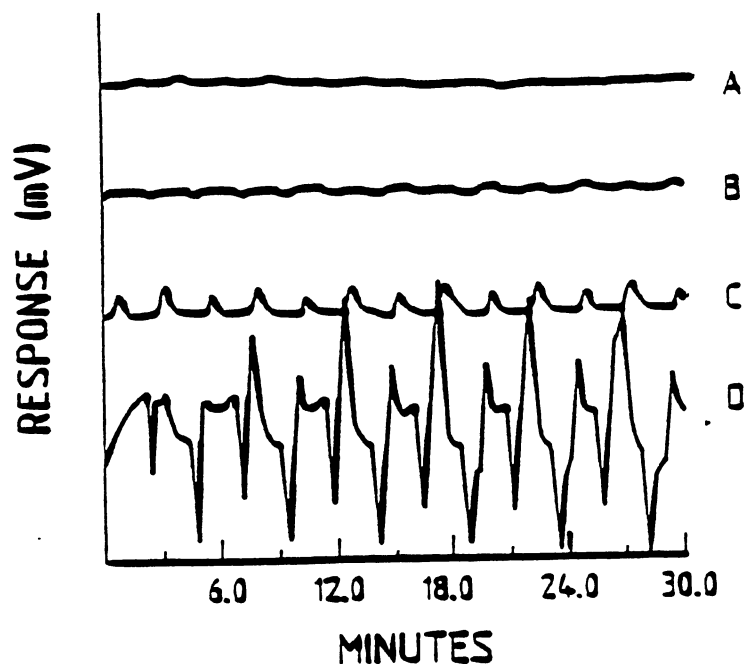


Figure 5. Mixing pattern of benzene and methanol with different mixing designs. (A) Condition as in C, 20- μ m capillary introduced; (B) condition as C, 2- μ m stainless steel frit introduced to each of three ports of the T; (C) condition as in D, pulsless flow; (D) special T, volume=30 nl, flow rates for two inlet ports= μ l/min. (ref. 53)

(pump pulsations) are a characteristic of reciprocating piston pumps, and for a given high-performance pump the magnitude of these changes will depend on the operation of the check valves, which usually improves with backpressure. These pulses cause nonuniform mixing of the reagent and eluent and produce a noise pattern that is in phase with

piston movement. This pattern is illustrated by data reported by Kucera and Umugat [53], as shown in Figure 5.

These authors studied the efficiency of a special T for the mixing of methanol and a 0.1% solution of benzene in methanol. The T was laser drilled to 150- μm ID, and the total volume was about 30 nl. A reciprocating pump was used for addition of both the eluent and the reagent, and figure 5 shows that quite large spikes in the baseline were observed due to pump pulsation; the majority of the pulsations were likely caused by the reagent pump as it would not have been operating against any significant backpressure.

Unfortunately, neither the backpressure absorbance nor the absorbance setting for the detector were given, but the data still clearly show that simple changes to the mixer have large effects on the background noise. Figure 5 shows that the addition of pulse dampeners reduced the noise, and further improvements were obtained by the addition of frits and a 20- μm capillary. These later improvements were likely due to improved pump performance as a result of increased backpressure; it is unlikely that improved mixing was an important factor as the volume between spikes about 100 μl and the volume inside the mixer was less than 30 nl

Two new approaches that are under investigation at the present time look promising for the reduction of pump pulses; these are the use of a hollow fiber PCR for reagent addition and a coincidence background correction technique.

The annular fiber devices developed by Dasgupta (43,54) look very promising because of their low dead volume and rapid mass transfer. Dionex markets a fiber device for reagent addition, but it has a relatively large volume of 100 μ l. Both these systems rely on the infusion of a pressurized reagent solution through pores in the membrane into the eluent. Which is flowing through the center of membrane. An attractive feature of these membranes is that their flexibility may help to dampen small pressure pulses, and thus they may give reduced baseline noises; further assessment of these devices is required to establish their performance. In coincidence background correction, the baseline noise is simultaneously monitored at two domains (different wavelengths for absorbance), one that gives a response for the analyte and another that gives a response to some other component, such as the reagent. The latter response can be used to monitor baseline noise due to poor mixing from both the mixer and pump pulses, and through appropriate normalization this chromatogram can be subtracted to eliminate baseline noise. Work by Cassidy and Elchuck (52) has shown that this procedure can eliminate noise by up to fivefold, but its practical application has some limitations. A data processing is required, and simultaneous signal measurement is required. Further work is required to fully assess the usefulness of this approach.

Chemistry

Introduction

The following section discusses the different chemistry principles of the inorganic PCR systems for the cation detection that have been reported in the literature to date. These systems have been organized chronologically within each of the different detection modes (absorbance, fluorescence, and so on) discussed.

Cation Detection

Most of the PCR chemistry developed for the detection of inorganic cations relies on the formation of metal chelates. Chelating agents have a number of properties that make them attractive for the PCR detection of metal ions:

1. Many metal chelates exhibit strong absorbance in the UV and visible region and thus can be measured with commonly used absorbance detectors. Absorbance in the visible region is often preferred because the background absorbance from reagents and other eluent components is normally less of a problem.
2. Metal chelate chemistry has been studied extensively and is well known for many metal chelate system.
3. Detection selectivity can be varied by the selection of chelating reagent or by the use of masking reagents.
4. Many metal chelate reactions are fast and essentially complete on mixing; thus delay systems, that can lead to

peak broadening if not used properly, are usually not needed.

Absorbance Detection

In one of the first applications of chelating reagents to the detection of metal ions, Kawazu and Fritz [33] examined 4-(2-pyridylazo) resorcinol (PAR) for the detection of Cd(II), Zn(II), Fe(III), Pb(II), Cu(II), Co(II), and Mn(II) eluted from a cation-exchange column. This reagent was added to the eluent (aqueous acetone or 2-propanol) as a dilute solution (0.01-0.2%) in strong ammonia (0.5-1.0 mol/liter). This medium-resolution system appeared to work well, but the performance of PCR system was not discussed.

One of the attractive features of PCR detection is the ability to quickly change the chemistry of the PCR system and thereby alter selectivity or sensitivity. This feature was illustrated during a study of the determination of trace elements in UO_2^{2+} [52]. The uranium in these samples reacted with PAR to give a large peak that interfered with the determination of the trace metal impurities; this is illustrated in Figure 6. Addition of carbonate as masking agent resulted in the formation of the stable uranium carbonate complex and prevented the reaction between uranium and PAR, as illustrated in Figure 7. The splitting of the Cu(II) peak was a result of poor chromatography due to the presence of large amounts of uranium under the Cu(II) peak.

The carbonate had very little effect on the reactions between PAR and the other transition metal ions studied.

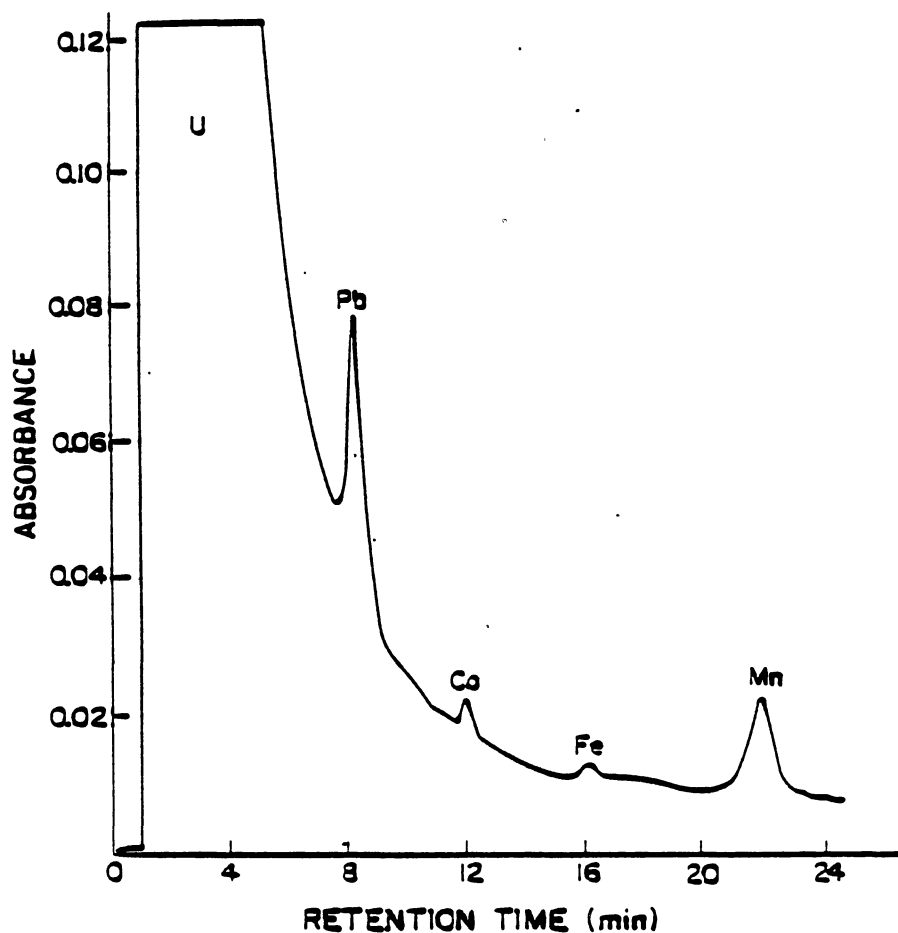


Figure 6. HPLC analysis of uranium. Experimental conditions; sample, 10 μ l of 357 mg/ml uranium solution. Aminex column; eluent, linear gradients from 0.3 to 0.5 mol/liter tartrate (pH 3.5) over 15 min; eluent flow, 1 ml/min, detection at 540 nm, post-column reagent, 50 μ g/ml PAR solution in 2 mol/liter ammonia and 1 mol/liter ammonium acetate. (ref. 52)

Most application of metal chlates for the absorbance detection of metal ions have relied on the measurments of the UV-visible absorbance of metal chelate. Recently, a somewhat different approach was taken for the application of metal chelate reactions to the PCR detection of the metal

ions [49,55]. These authors note that the optimum absorbance of metal chelates can vary significantly from metal to metal, and thus it may not be possible to obtain optimum sensitivity for all the metal ions of interest. Consequently it was suggested that one should measure the decrease in absorbance of the chelating reagent as quantitative measure of the metal ion present.

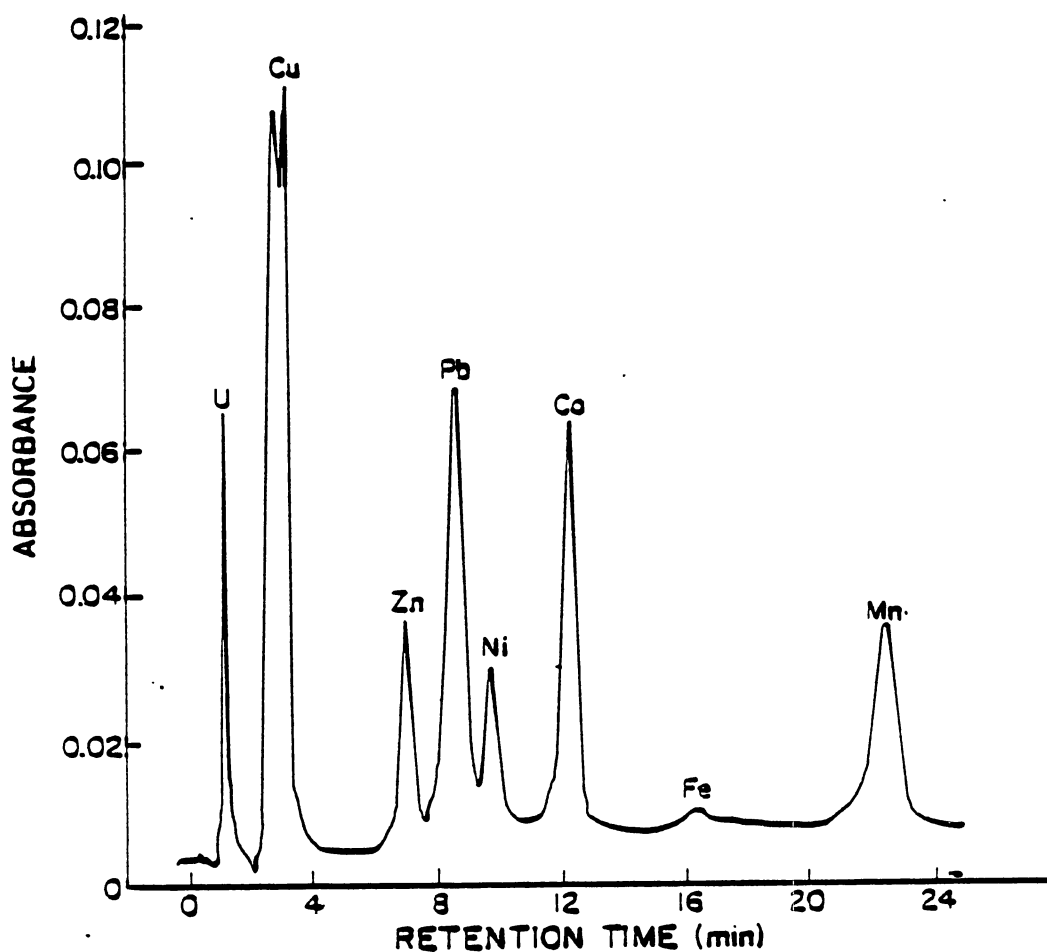


Figure 7. HPLC analysis of uranium with 0.3 mol/liter carbonate in post-column reagent solution. Experimental conditions as in Figure 6. (ref. 52)

In these studies, dithizone and eriochrome black-T were used. A reaction coil (1.5 m X 0.3 mm ID) was used to allow

sufficient time for the metal complexes to form, but neither the reaction kinetics nor the performance characteristics of the reaction coil were discussed.

Electrochemical Detection

In 1973, Takata and Arikawa published the first in a series of papers on the separation of metal ions by HPLC [56]. This paper described a PCR system for electrochemical detection that was based on coulometric detection after the following exchange reaction:



The liberated Hg(II) ions were measured by their reduction in a coulometric detector with an electrolytic efficiency of >99.5%. This system was applied to the following metal ions: Ag(I), Au(III), Bi(III), Cd(II), Co(II), Cu(II), Fe(II), Fe(III), Hg(II), Mn(II), Ni(II), Pb(II), VO₂(II), Zn(II), and ions of alkaline earth metals and rare earth metals.

With this type of exchange reaction it was possible to detect this wide variety of metal ions without any interference from dissolved oxygen. In a later report [57], Takata et al. studied the exchange reaction with Hg(II)-EDTA or DTPA as the basis of a PCR coulometric detector for metal ions; the Hg(II) complex was preferred as its use reduced the interference from dissolved oxygen. However, from an environmental viewpoint the authors recommended the use of

Cu-DTPA in spite of its lower sensitivity (by a factor of approximately 2).

The decrease in the anodic diffusion current of EDTA at a dropping Hg electrode has been used [46] as the basis for the detection of rare earths as they eluted from a medium-resolution column (25- μ m cation resin). The cell volume was quite large (1 ml), and detector sensitivity appeared to be poor relative to other electrochemical and absorbance PCR systems reported for lanthanide detection [36,23].

In an extensive report (approximately 200 pages) by Dorey [58], the potential of a Cu(II)-specific ion electrode has been examined as a PCR detector for lanthanide and first-row transition metal ions. The principle of the detection was similar to that used by Takata, liberation of a metal ion [Cu(II)] from an EDTA complex by the eluted metal ions [56]. However, almost all of the report was devoted to studies on the characteristics of the electrode response under a variety of conditions, and there were no reported applications with a chromatographic column

Fluorescence and Luminescence Detection

Hartkopf and Delumyea [59] have examined the potential of the luminol reaction for the PCR determination of metal ions with a fluorescence detector, but a column was not used in this evaluation. A number of metal ions catalyze the oxidation of luminol (5-amino-2,3-dihydro-1,4-phthalazinedione) to form 3-aminophthalic acid in an excited

state, which will then decay to the ground state via photon emission. The chemiluminescence produced is proportional to the metal ion concentration over a wide range, and the reaction has been used for the quantitative determination of a number of metal ions. The PCR system used here is not suitable for HPLC due to its large dead volume (8 ml); however, it does illustrate the potential of such an approach. The sample was mixed with luminol and then with hydrogen peroxide before entering the photomultiplier detection chamber. Co(II) gave a linear calibration curve, but the curve for Cu(II) was nonlinear. The estimated detection limits for a number of metal ions varied from 6×10^{-5} to 7×10^{-11} g, which for most metal ions is not significantly better than that obtained by other PCR detection techniques. No applications were reported, but all the above metal ions were detected quantitatively and examples of linear calibration curves were given. Aluminium and antimony were also detected, but not quantitatively.

Beckett and Nelson [60] have investigated a fluorescence PCR technique for the determination of metal ions. To provide a uniform response for a variety of metal ions the metal ions were separated as 4-aminophenylene-diaminetetraacetic acid chelates, and then the eluted chelates were converted into fluorescence derivatives with fluorescamine. The chelates exhibited a linear fluorescence response from 5×10^{-11} to 5×10^{-7} g of metal ion injected onto 10- μ m bonded phase anion-exchange column. The

detection limits for a $S/N = 2$ were 80 pg for Pb, 80 pg for Cd, and 60 pg for Zn. These detection limits are superior to those reported for other PCR systems, but there are two disadvantages associated with this procedure. The first is the necessity to prepare the chelates prior to injection, which will complicate the analysis and reduce accuracy. The second is that it may be difficult to separate a wide variety of metal ions by this procedure because of the chemical similarity of the different chelates or the dissociation of the chelates during separation; these types of separation problems are observed for the separation of EDTA metal chelates.

Spectrometric Detection

The most popular spectrometric detectors for metallic species used in HPLC have included flame atomic absorption (FAA), graphite furnace atomic absorption (GFAA), and the plasma emission detectors (PED). Reaction detectors for spectrometric detectors have included solvent extractors, aerosol desolvators, and hydride generators. Their primary purpose has been to ameliorate the compatibility problems associated with introducing a liquid sample to a high-temperature source. The ultimate goal of each reaction system is to efficiently condition the sample to enhance analyte transfer to the atomizer while maximizing sensitivity and avoiding adverse interference effects. Both the FAA, GFAA, and PED have achieved considerable success as

HPLC detectors, but there have been relatively few application reported for spectrometric PCR systems. (61-64).

Applications

Cations

Absorbance

Alkaline earth and transition metal ions: Fritz has always been prominent in the development of inorganic LC, and in 1973, he and Kawazu [33] were the first to apply an absorbance PCR system for the LC determination of metal ions. This system used a 250-350 mesh cation resin and thus is, by today's standards, a low-resolution system; however, the procedures used here formed the basis of many further studies by both these and other workers. The color-forming reagent PAR was used for the detection of Cd(II), Fe(III), Pb(II), Cu(II), Co(II), Zn(II) and Mn(II). This reagent was added to the eluent (aqueous acetone or 2-propanol) as a dilute solution (0.01-0.2%) in strong ammonia. The PCR system appeared to work well, but its performance was not discussed. The main purpose of this paper was to develop the chromatographic conditions required for the separation of these metal ions. Linear calibration curves were obtained for Cd(II), Zn(II), Fe(III), Pb(II), Cu(II), and Co(II), but Mn(II), always eluted as a double peak.

Fritz and Story [24] examined the potential of PAR, arsenazo-I, and arsenazo-III as PCR reagents for a number of

metal ions. Separations were done on specially prepared low-capacity cation-exchange resins, which provided rapid separations in spite of their large particle size. This paper focused on the following separations: Th (IV) from La(III); Th(IV) from Zr(IV); Ca(II) from Mg(II); Zn(II), Pb(II), Cu(II), Mn(II), and Ni(II) from each other; and Pb(II) from large amounts of other divalent metal ions. Analysis were performed on two NBS metal standards for Pb(II), Zn(II), and Ni(II) in the 0.9-5.0% range; the LC results and the NBS values agreed to within 0.2-0.4%.

Kawazu [65] used a PCR with PAR to detect the metal ions Cd(II), Zn(II), Fe(III), Pb(II), Cu(II), U(VI), Co(II), Fe(II), Mn(II), V(VI), and Ni(II). The author used a long PTFE tube to ensure reaction between the metal ions and the PCR reagent. This and the large dead volume in the detector cell (90 μ l) would have limited the resolution obtained with the smaller packings studied (13-17 μ m) and certainly would not be suitable for the small-particle packing available today. The main purpose of this paper was to compare the behavior of a number of cation-exchange resins and to examine briefly the use of on-column preconcentration for trace metal ion analysis. The sample size used was 60 ml, and the amounts of metal ions in the sample were in the range of 5×10^{-5} to 1×10^{-8} mole.

Cassidy and Elchuk [42] have used PCR detection with trace enrichment for the determination of transition metal ions at ng/ml and pg/ml concentration levels. An inert

sampling system was used to introduce on-line enriched samples to HPLC ion-exchange columns (5- and 10 μm bonded phases and 13- μm resin cation exchangers). The PCR, which used a PAR reagent solution, did not contribute to band broadening, and column efficiencies (HETP) were in the range of 0.1-0.4 mm for flow rates of 2-4 ml/min; column efficiencies were quite dependent on the metal ion and the chelating agent used for elution. The background noise was 2×10^{-4} absorbance units, with a PAR reagent solution that gave a background absorbance of 0.02 units. Over 50 metal ions were tested for a reaction with PAR under the conditions used for detection (2×10^{-4} M PAR in 2.0 M ammonia and 1.0 M ammonium acetate).

In other studies reported by Cassidy and Elchuk [52], a PAR PCR was used with a 13- μm ion-exchange resin for the determination of trace metals in materials used in the nuclear industry, such as steels, Ni-Cr-Fe alloys, zirconium and uranium. This work showed that in many instances HPLC could be applied to trace metal ion determinations in complicated matrices without preliminary treatment of the sample. A number of standard metals were analyzed by this technique. These analyses were difficult to do by standard spectroscopic methods because of spectral interferences and matrix effects. The results of this study showed that the selectivity and sensitivity of PCR detection permitted the direct application of HPLC to these types of analyses without any sacrifice in accuracy.

A PCR based on a reaction with PAR was applied to the determination of trace concentration of metal ions in groundwaters within and external to a waste-management site at a nuclear research establishment [66]. At this site the behavior of inactive Co(0.1-2.0 pg/ml) and ^{60}Co , which was present in very small concentrations, were of particular interest. Predictions of the environmental fate of ^{60}Co and other dissolved metal ions is of importance to the evaluation of possible release from nuclear waste repositories. Direct analysis of the metal ions in these groundwaters was impossible by most analytical techniques for traces, but the combination of the sensitivity of an absorbance PCR with trace enrichment offered the potential of both determining and speciating the dissolved metal ions. Trace enrichment procedures were used to analyze a large number of samples over a considerable time period, and the relative standard deviations observed were in the range of 2-10% for the concentration range of 1-500 ng/ml.

An absorbance PCR based on the reaction of the metal ions with PAR was used to monitor the elution of metal ions during studies of new chromatographic techniques for the separation of metal ions [67]. Reversed phases that were either "permanently" coated with a C_{20} sulfonate or dynamically coated with lower molecular weight sulfonates were tested for the separation of transition metal ions. Because of the small dead volume [36] of the PCR used, it was possible to measure column efficiencies for 5- μm phases.

Peak symmetry and column efficiency were better than that obtained with either conventional resins or with bonded-phase exchangers, and efficiencies as low as 0.01 mm HETP were observed for the transition metals studied.

Lanthanides: In 1974, Story and Fritz [37] published an important paper on the separation of the lanthanides. Although it was a low-resolution separation by today's standards, it was of importance because it was the first reported separation of lanthanides with continuous on-line detection, and the results reported in their paper formed the basis of the approaches used by a number of workers to separate this important group of metal ions.

The first application of an absorbance PCR system to HPLC column (5- and 10- μ m bonded-phase exchangers and a 13- μ m resin) for the determination of the lanthanides was reported by Elchuk and Cassidy [36]. The system developed by Fritz was modified to make them more suitable for high-performance columns. The optimum reagent concentrations were found to be 2×10^{-4} M for PCR and 1.3×10^{-4} M for arsenazo-I. These concentrations gave linear working ranges of 10-600 ng. With this system it was possible to separate all the lanthanides in 18 min or less. The reproducibility obtained with this detection system for the gradient separation of 14 lanthanides (100 ng of each) ranged from 2 to 6%.

Knight et al. [68] have described the application of an absorbance PCR detector (based on arsenazo-III) for the HPLC

determination of lanthanides in irradiated thorium-uranium dioxide fuels. The PCR and dynamic ion-exchange system (separation was performed on a 5- μm C₁₈ reversed phase) offered a rapid and sensitive method for the determination of lanthanides. The sensitivity of the PCR (detection limits were about 2.5 ng for the lanthanides) permitted the direct determination of the fission monitor ¹³⁹La in dilute solutions of the irradiated fuel without preliminary sample clean up. Significant saving (up to a factor of 10) in time and analysis cost, relative to traditional isotope-dilution mass spectrometric techniques, were obtained without any sacrifice in precision or accuracy.

Actinides: Cassidy and Elchuk [69] have used a PAR-PCR in study of the potential of HPLC for the determination of U(VI) in ground waters and in urine; conventional resins (anion and cation) and bonded-phase resins were examined. The best chromatography was obtained on a bonded-phase cation exchanger with an α -hydroxyisobutyric acid eluent. The PCR detector was compared with an electrochemical detector, and the PCR system gave better sensitivity; the detection limit (2 X baseline noise) for 100- μl samples was 6 ng (60 ng/ml). In-line trace enrichment was used to decrease detection limits, and linear calibration curves were observed in the ranges studied: 0.5-50 ng/ml for ground water and 25-400 ng/ml for artificial urine.

The results of Knight et al. [68] have shown that U(VI) can be determined accurately by PCR-HPLC. A comparison of

the analysis results for a series of U(VI) samples by PCR-HPLC and coulometry showed that the agreement between the two methods was within 0.3% and that the relative standard deviation of the differences between these analyses was 0.9%.

Conclusions

The future of inorganic PCR systems will likely lie in the area of the determination of metal ions. The single-column and suppressed column "ion chromatography" systems are now the methods of choice for inorganic anion analyses, and PCR anion system will likely be required for only a few unique applications. These "ion chromatography" systems are not generally suitable for the determination of metal ions and unless new detector technology is developed, PCR systems will remain the method of choice for the detection of separated metal ions. In the present study a HPLC-PCR system is used to separate and detect trace quantities of U(IV) and U(VI) in aqueous samples.

CHAPTER III

EXPERIMENTAL

Direct Fluorometric Measurement Of U(VI) In Aqueous Solutions.

The measurement of fluorescence of uranium(VI) in phosphoric acid solution has been reported [70,71]. In these studies phosphoric acid was added to the uranyl ion solution after a separation step, a time consuming process.

In the procedure developed in this study, ammonium phosphate buffer solution is added directly to an aqueous sample solution containing uranium to enhance the fluorescence signal of the uranyl ion. The uranium concentration in aqueous solution is measured directly without the tedious and time consuming separation or pre-concentration steps.

Reagent and Materials.

Reagent grade chemicals and deionized distilled water (DDW) were used throughout the procedure. Ammonium phosphate monobasic, phosphoric acid, sodium bicarbonate, potassium sulfate, iron(II) and iron(III) nitrate, magnesium(II) sulfate, Manganese(II) sulfate, and calcium

nitrate were purchased from Baker Chemical Company. An uranium nitrate standard solution was purchased from Alfa Products.

Buffer-Complexing Solution.

The complexing solution was prepared by adding 230 g of ammonium phosphate and 45 ml of phosphoric acid to a 1000 ml volumetric flask. It was made up to the mark with DDW. The pH of the solution was adjusted to 4.30 with phosphoric acid. This solution in future references is the phosphate buffer.

Uranyl Nitrate Stock Solution.

0.2110 g of uranyl nitrate hexahydrate was dissolved into 100 ml volumetric flask and made up to the mark with DDW. The uranium(VI) concentration in the stock solution was 1000 ppm. Working standard solutions were then prepared from the stock standard.

Apparatus.

A Farrand spectrofluorometer equipped with a 150 watt DC xenon arc lamp, a RCA model 4840 nine stage side-on photomultiplier tube, a high speed picoammeter and a high voltage power supply model 204 from Precision Instrument were used for the fluorescence measurements. A schematic of the optical layout of the fluorometer is shown in Figure 8. To record the peaks a Sargent-Welch recorder was used.

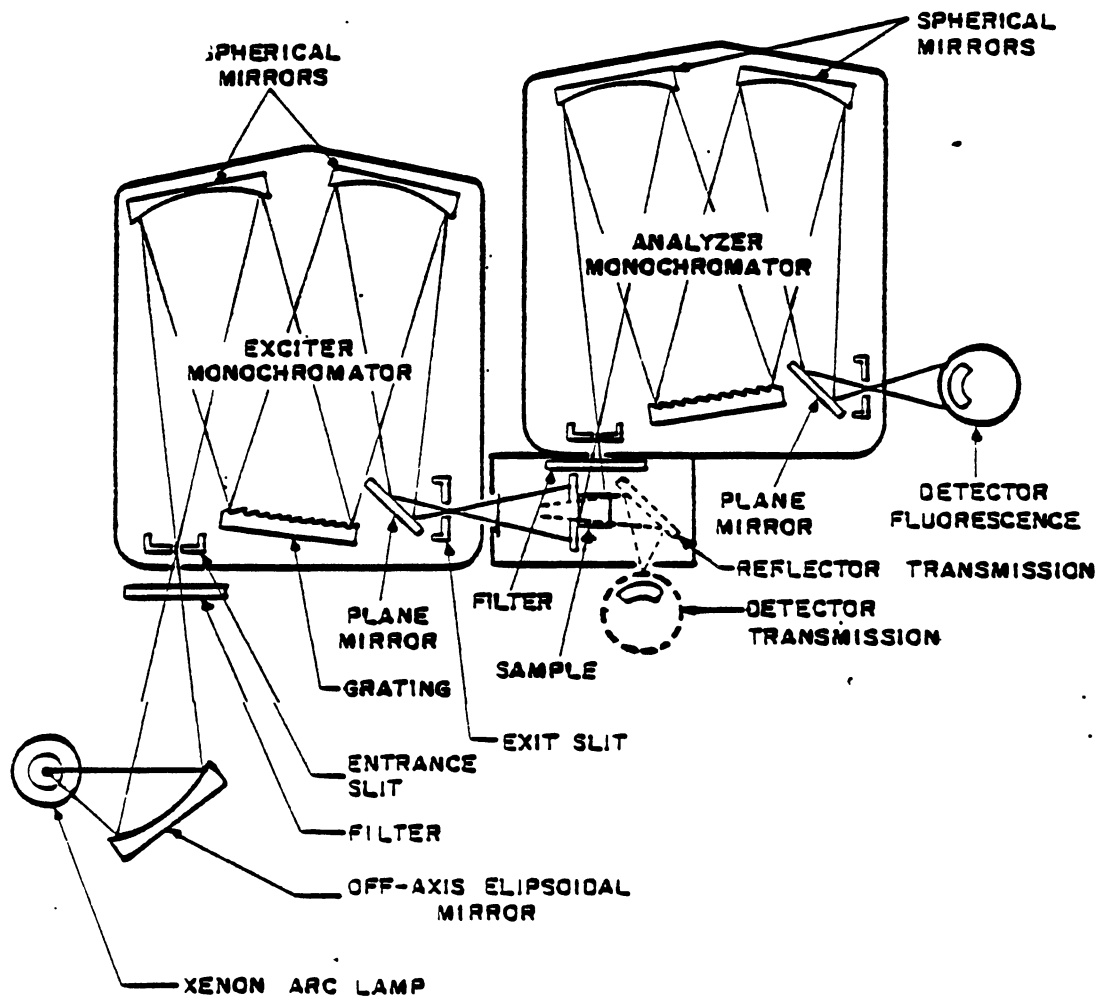


Figure 8. Optical Diagram of Spectrofluorometer

Limit of Detection and Calibration Curve.

An aliquot of slightly acidic standard solution (pH 6-6.5) containing uranyl ion was transferred to a 100 ml volumetric flask, then 30 ml of the phosphate buffer solution was added and the solution was made up to the mark with DDW.

A cuvette with 1 cm path-length was used for all the fluorometric measurements. The emission spectra of the sample was scanned from 400 to 600 nm with an excitation setting at 285 nm. The excitation and emission spectra of U(VI) is shown in Figure 9.

A calibration curve was obtained using varying concentrations of uranyl nitrate standard solution. Solutions containing 50, 100, 150, 200, 250, 300, 350, and 400 ppb of uranyl ion were prepared from the stock standard solution.

All of the uranium solutions were excited at 285 nm and the fluorescence signals were measured at 525 nm, the strongest of the triple peaks for the uranyl ion.

Figure 10 shows a calibration curve for the uranyl nitrate solution.

The limit of detection was obtained by two methods. First the detection limit was calculated according to the method of three times standard deviation of intercept (background noise).

$$\text{L.D.} = X_{\text{blank}} + 3 \times \text{sd}_{\text{blank}}$$

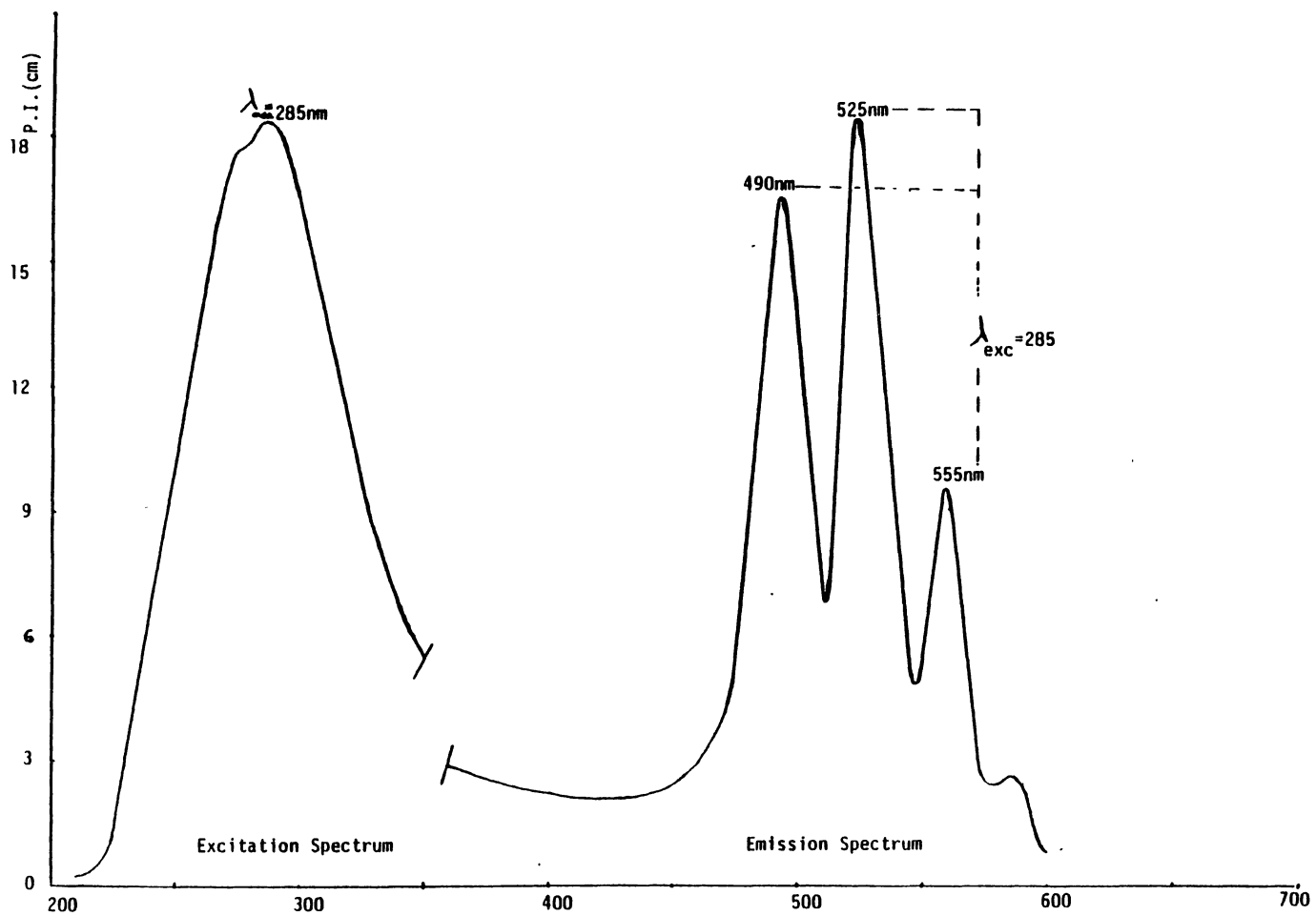


Figure 9. Excitation and Emission Spectra of an Aqueous Solution of $\text{UO}_2(\text{NO}_3)_2 \cdot 6\text{H}_2\text{O}$

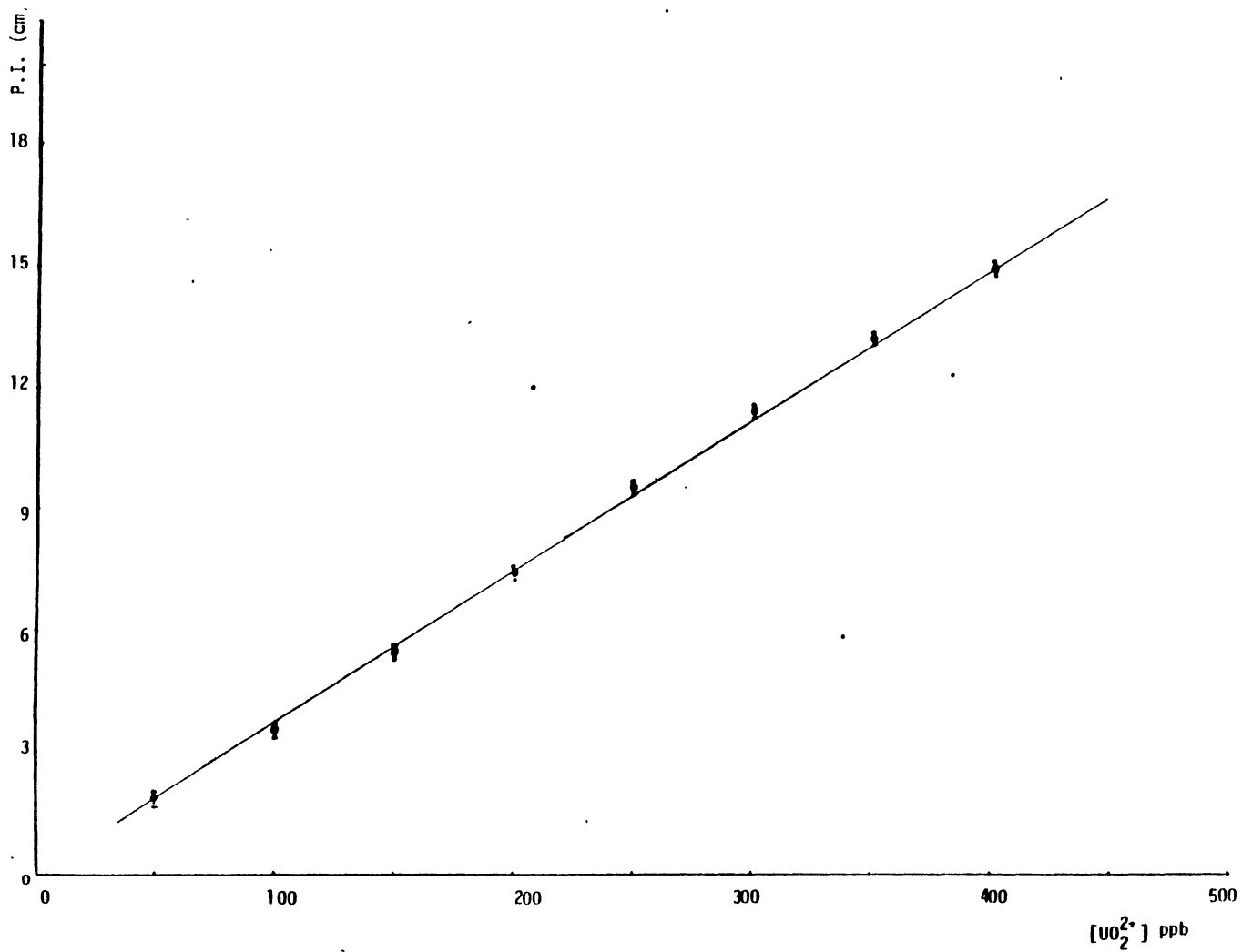


Figure 10. Typical Calibration Curve for Uranyl Nitrate Solution

To calculate the detection limit with the second method, the sensitivity of the fluorometer was set such that the recorder started recording noise when the cuvette was filled with buffer solution. Then an increasing amount of uranyl nitrate solution was added until the height due to UO_2^{2+} ion was twice as high as the noise peaks. Figure 11 shows signal-to-noise ratio of 1 ppb U(VI) solution.

Dependence of The Fluorescence Signal on Uranyl Ion Concentration and On The Amount of Buffer Solution Added.

The gain of the photomultiplier tube was adjusted with the picoammeter so that the fluorescence measurement did not deflect the recorder pen by more than two thirds of full scale. The instrument was rezeroed with ammonium phosphate buffer at $\lambda_{\text{exc}}=285$ and $\lambda_{\text{em}}=525$ nm. Varying volumes of buffer were added to fixed amounts of uranyl ion (usually 2 ppm) and the fluorescence signal was measured after the solution was mixed and placed in the cuvette. Figure 12 shows the fluorescence intensity of the uranyl ion as a function of volume of buffer added.

After obtaining the optimum buffer volume, it was necessary to measure the fluorescence intensity of the uranyl ion as a function of uranium content. Again the photomultiplier gain was adjusted so that the fluorescence measurement would not deflect the recorder pen more than two thirds its full scale. The instrument was then re-zeroed with the buffer solution. An appropriate amount of standard

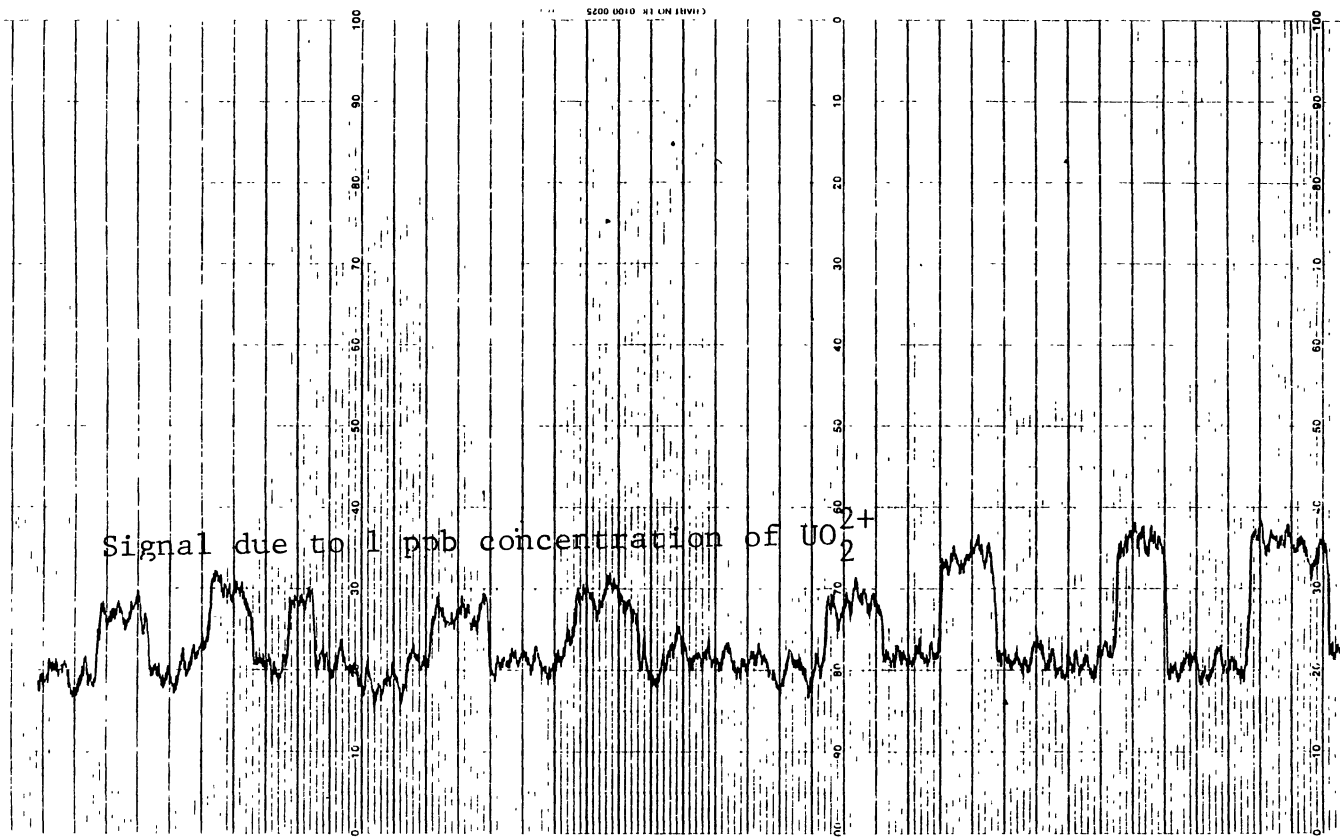


Figure 11. Limit of Detection for Uranyl Ion Using Signal-to-Noise Ratio Method

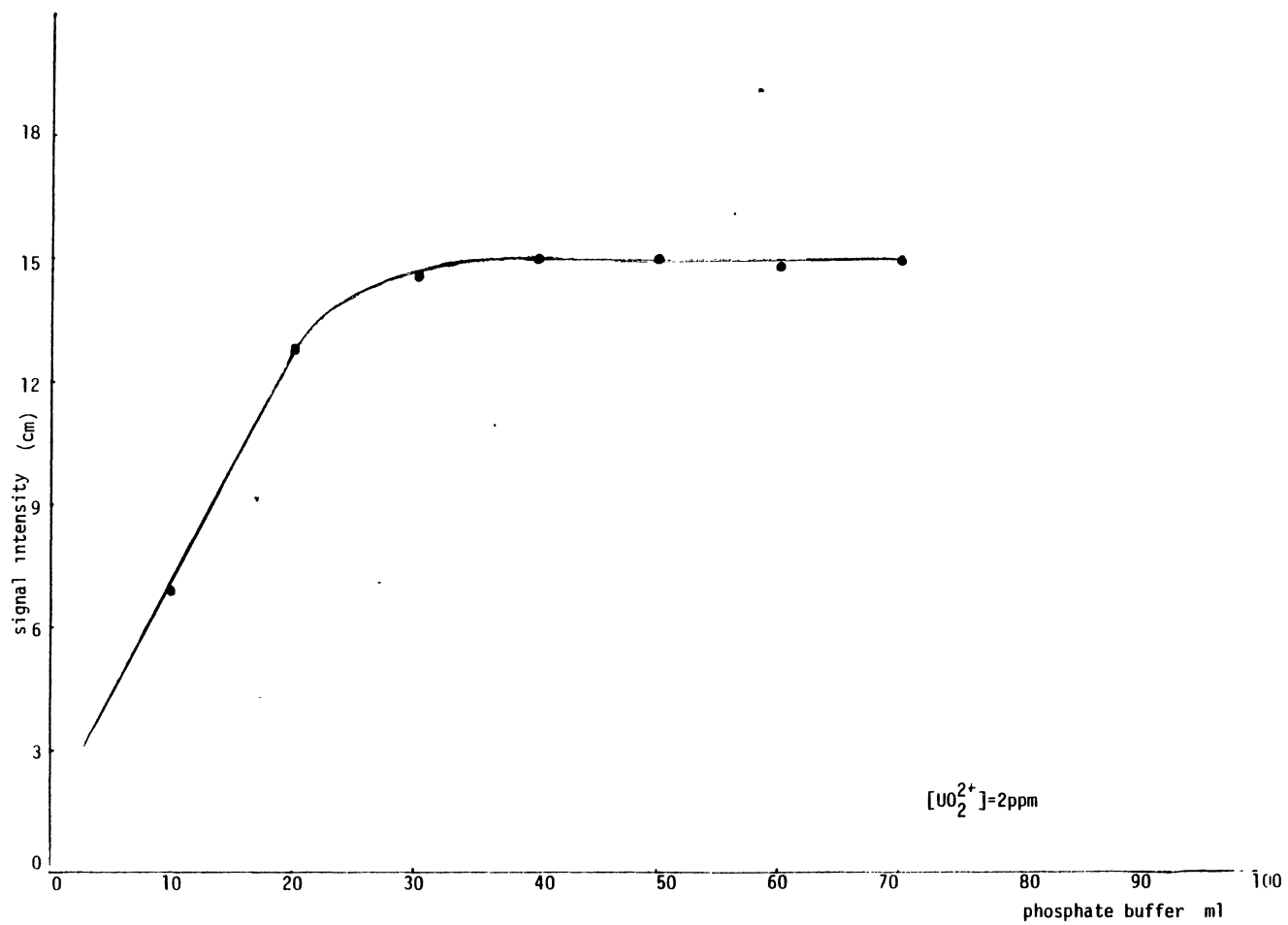


Figure 12. Fluorescence Intensity of Uranyl Ion in Phosphate Buffer as a Function of Buffer Content

uranium solution (0.5 to 50 ppm) was added to 30 ml of buffer solution and made up to 100 ml with DDW. A final fluorescence measurement was made after the solution was mixed and placed in the cuvette. Figure 13 shows the fluorescence intensity of uranyl ion as a function of uranium content.

Interferences by Cations.

Cations such as Na^+ , K^+ , Mg^{2+} , Fe^{3+} , and Ca^{2+} , are commonly present in natural waters. Their concentration levels usually are high enough to interfere with direct determination of uranium in water samples (72).

The effect of the above cations on the direct fluorometric determination of uranium was examined by applying the method to fixed amount of uranium (usually 2 ppm) in the presence of varying quantities of the ions being studied.

A 1000 ppm stock solution of each cation was made. An appropriate amount of stock solution of each cation was added to a 100 ml volumetric flask containing uranium(VI) solution (2 ppm). Then it was made up to volume with DDW and the fluorescence signal was measured in a 1-cm cell. Figures 14, 15, 16, and 17 shows the plot of the fluorescence signal intensity of uranyl ion as a function of interfering cations.

The relative peak intensity was calculated by dividing peak height in the presence of interfering ions by that of

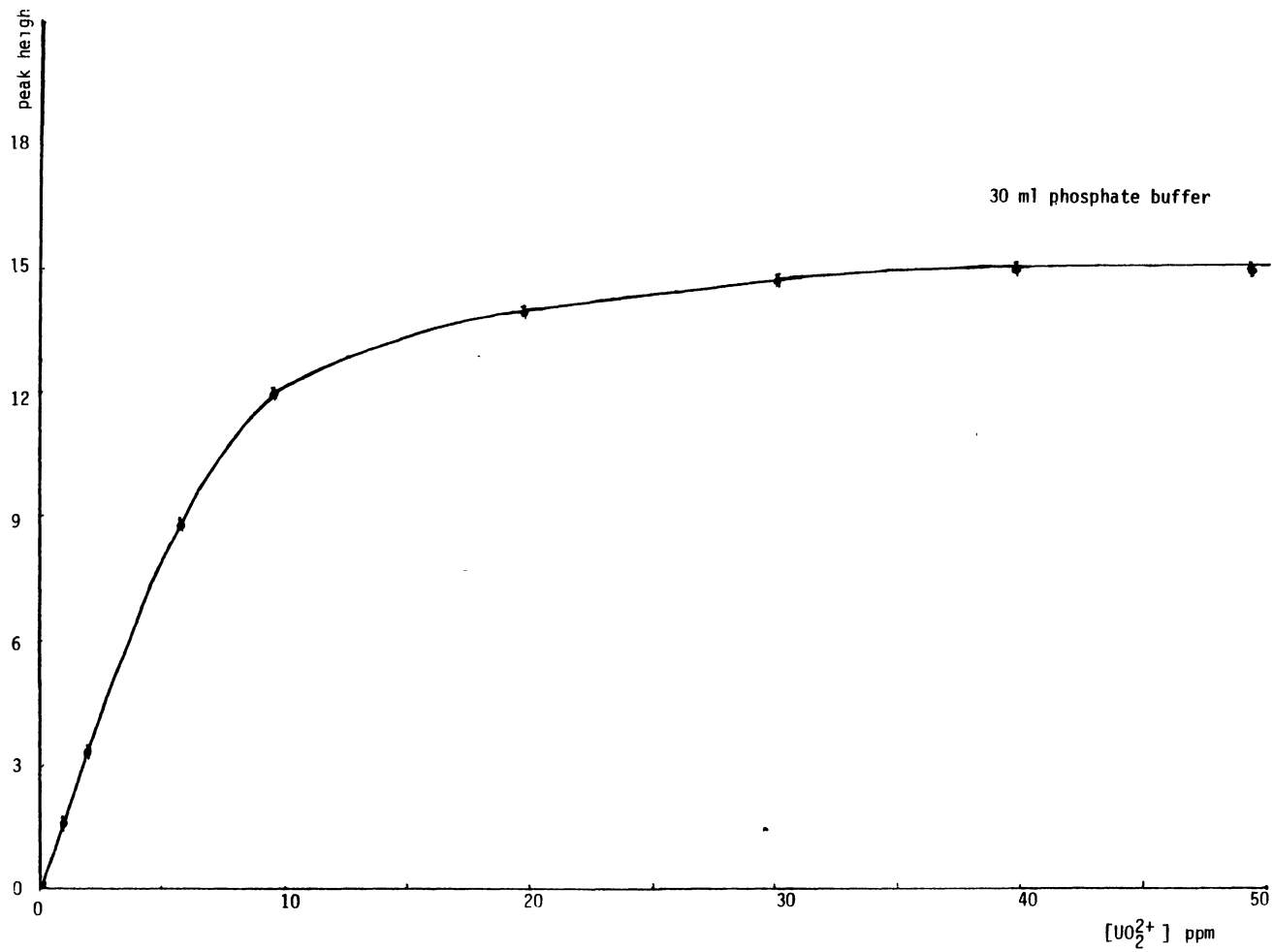


Figure 13. Fluorescence Intensity of Uranyl Ion in 30 ml Phosphate Buffer As a Function of Uranium Content

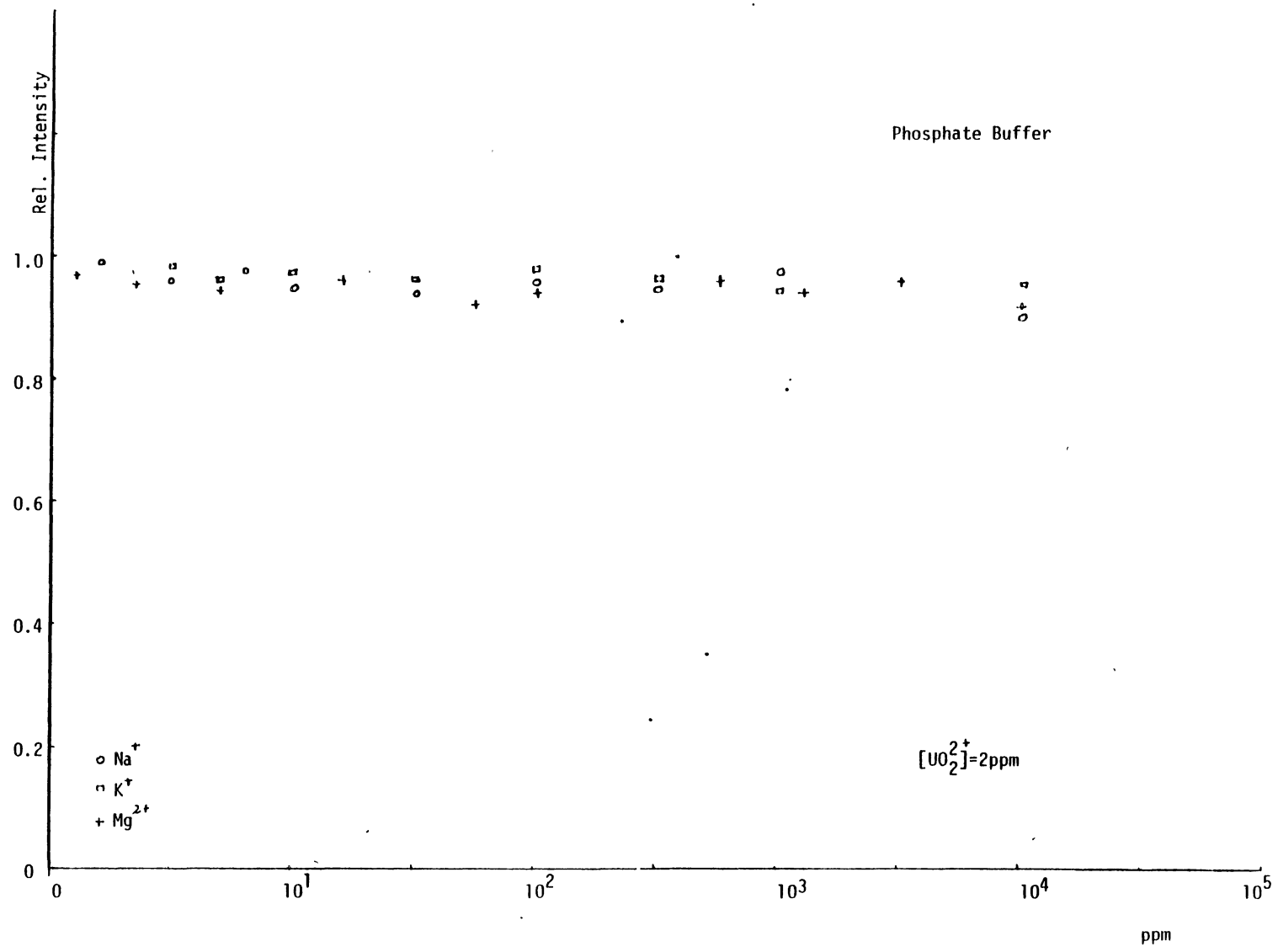


Figure 14. Fluorescence Intensity of Uranyl Ion in Phosphate Buffer As a Function of Na⁺, K⁺, and Mg²⁺ Concentrations

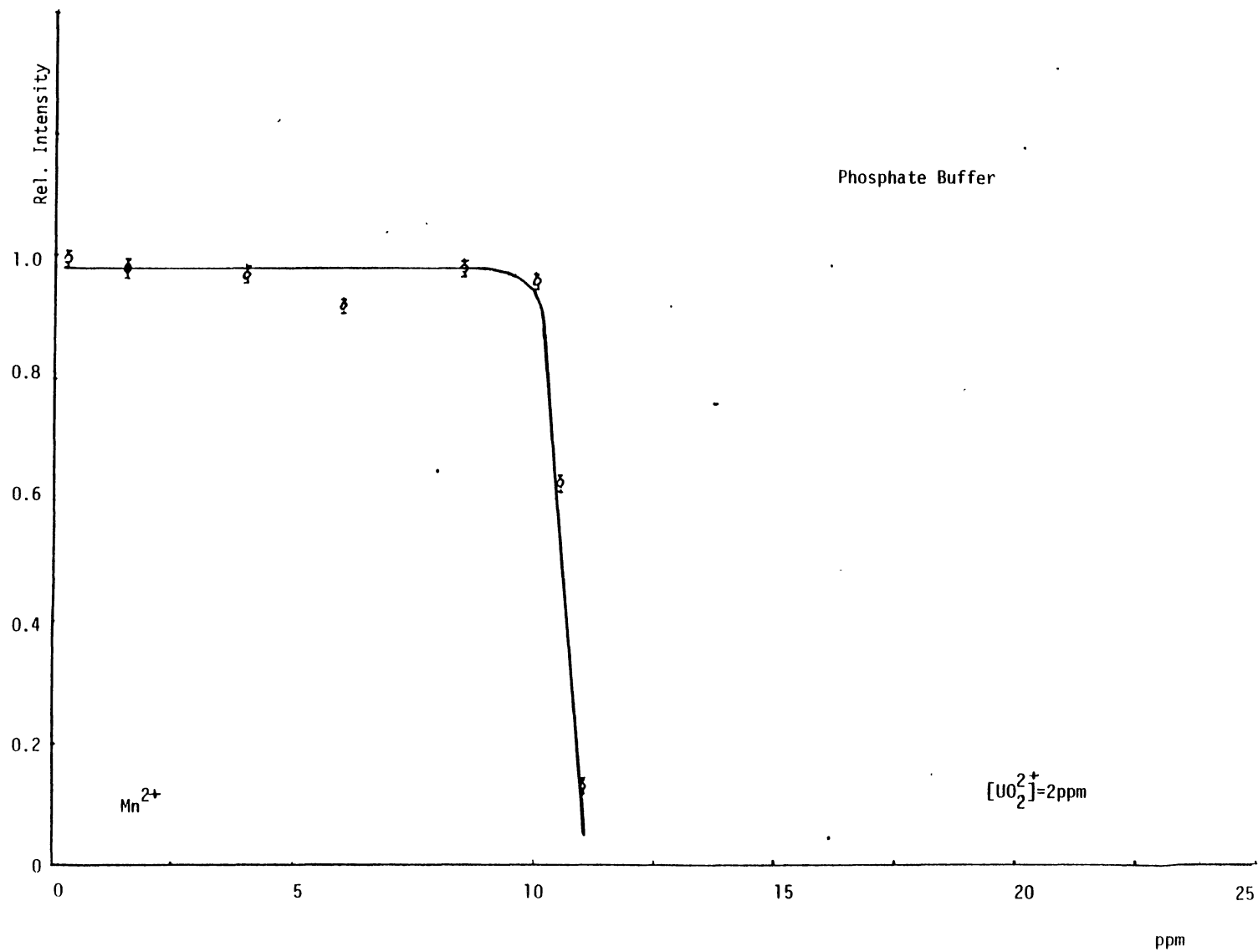


Figure 15. Fluorescence Intensity of Uranyl Ion in Phosphate Buffer As a Function of Mn^{2+} Concentration

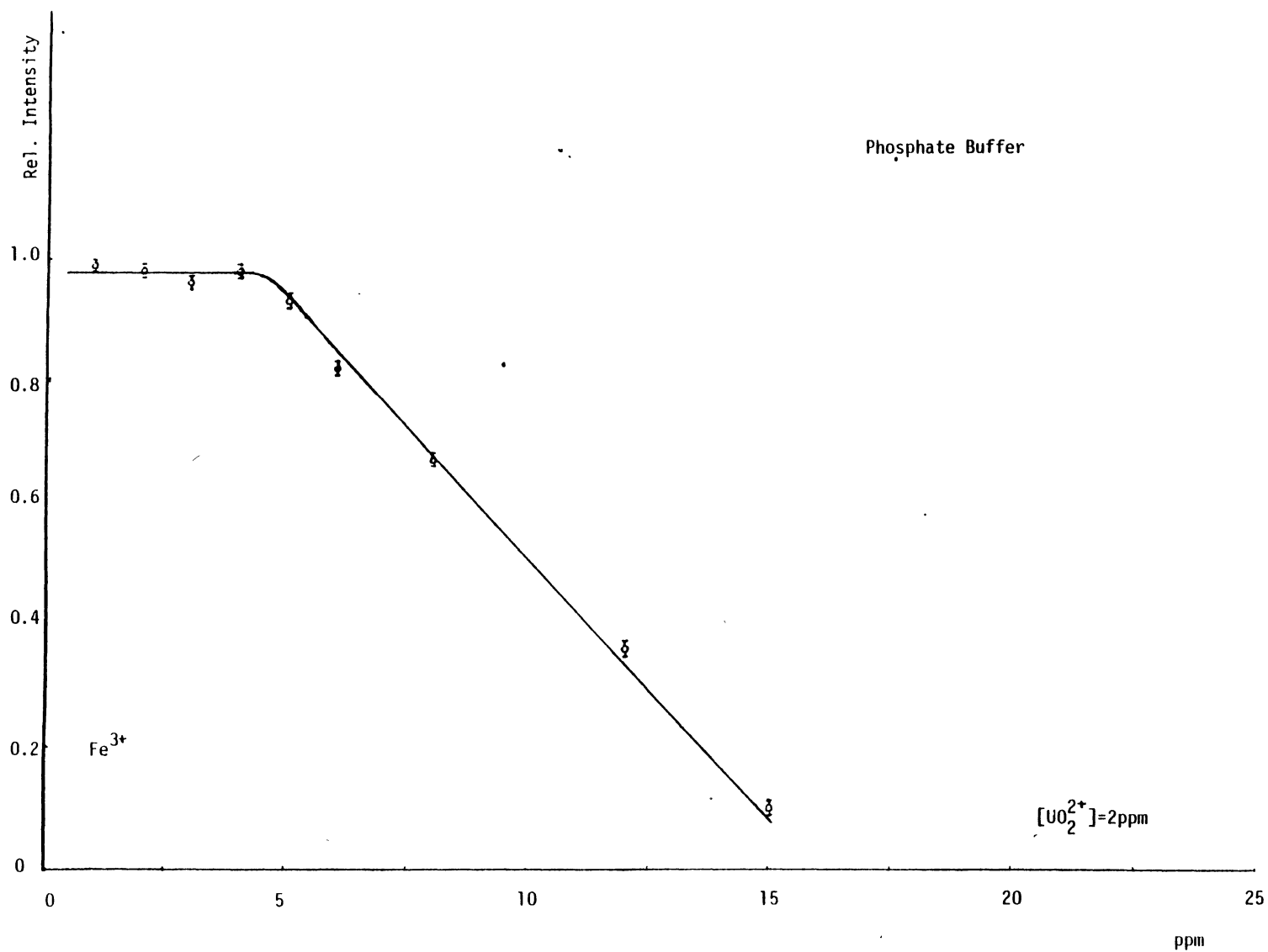


Figure 16. Fluorescence Intensity of Uranyl Ion in Phosphate Buffer As a Function of Fe^{3+} Concentration

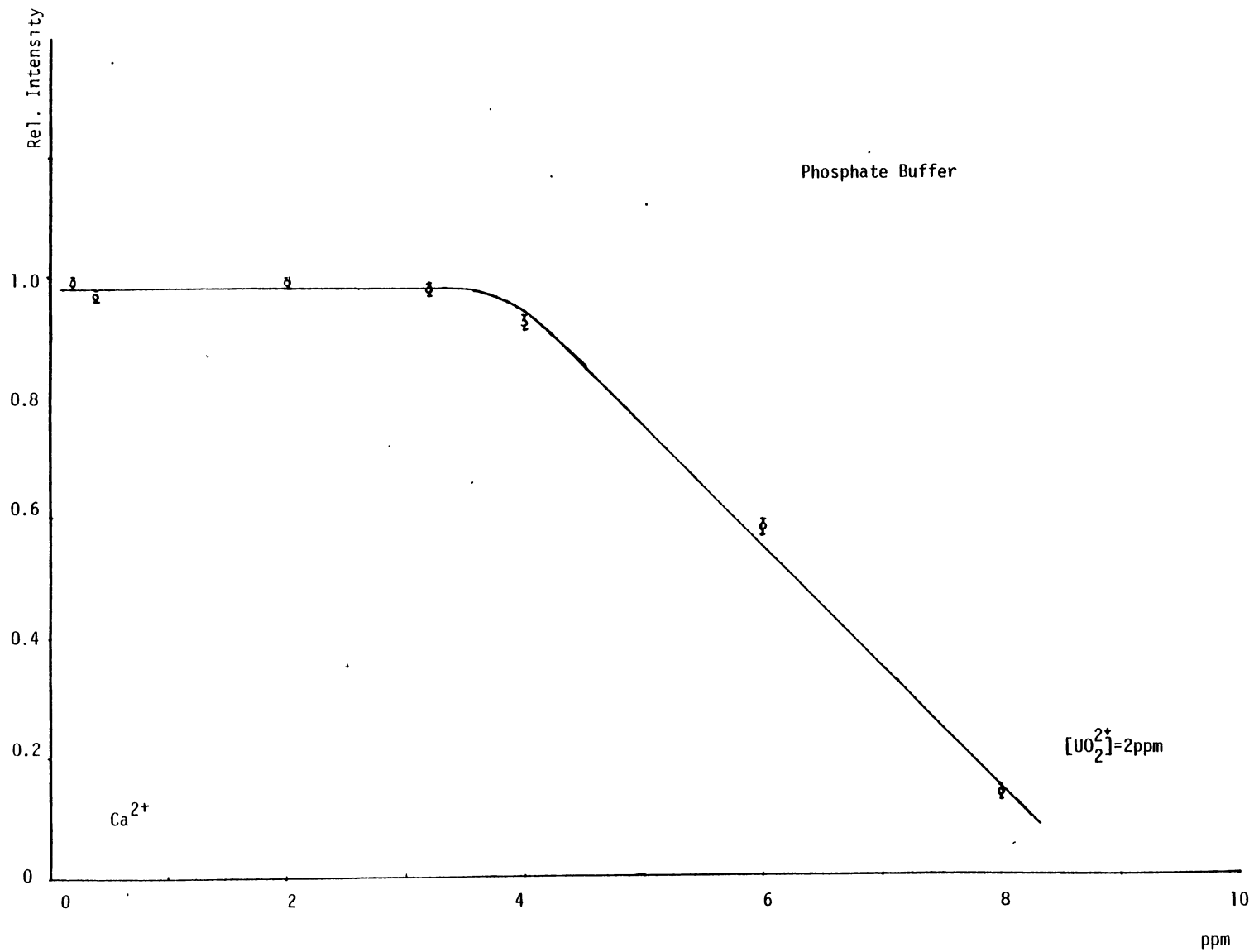


Figure 17. Fluorescence Intensity of Uranyl Ion in Phosphate Buffer As a Function of Ca^{2+} Concentration

in absence of interfering cations. The value of relative intensity for uranyl ion in the absence of interfering ions is one or 100 on the percent basis.

Interferences by Anions.

The common anions present in natural waters in concentration high enough to interfere with uranium determination are $\text{CO}_3^{=}$, $\text{SO}_4^{=}$, NO_3^- and Cl^- .

To find the answer to the quenching problem of fluorescence signals due to the presence of anions in water samples, increasing quantities of the ions were added to a fixed amount of uranium (2 ppm) and the fluorescence signal intensity was measured.

A 10,000 ppm stock solution of each anion was made. An appropriate amount of stock solution of each anion was added to a 100 ml volumetric flask containing 2 ppm of uranyl ion solution. Then the volume was made up with DDW. The fluorescence signal was measured as before (explained for cations).

Figure 18 shows the plot for the dependence of the fluorescence signal on the concentration of the main anions expected in natural water. Figure 19 shows the fluorescence intensity of the uranyl ion as a function of Cl^- ion.

HPLC Separation And Post-Column Fluorometric DeterminationOf U(VI) In Aqueous Solutions.

The separation of U(VI) on cation exchange columns has been reported [68]. A PCR based on a reaction with

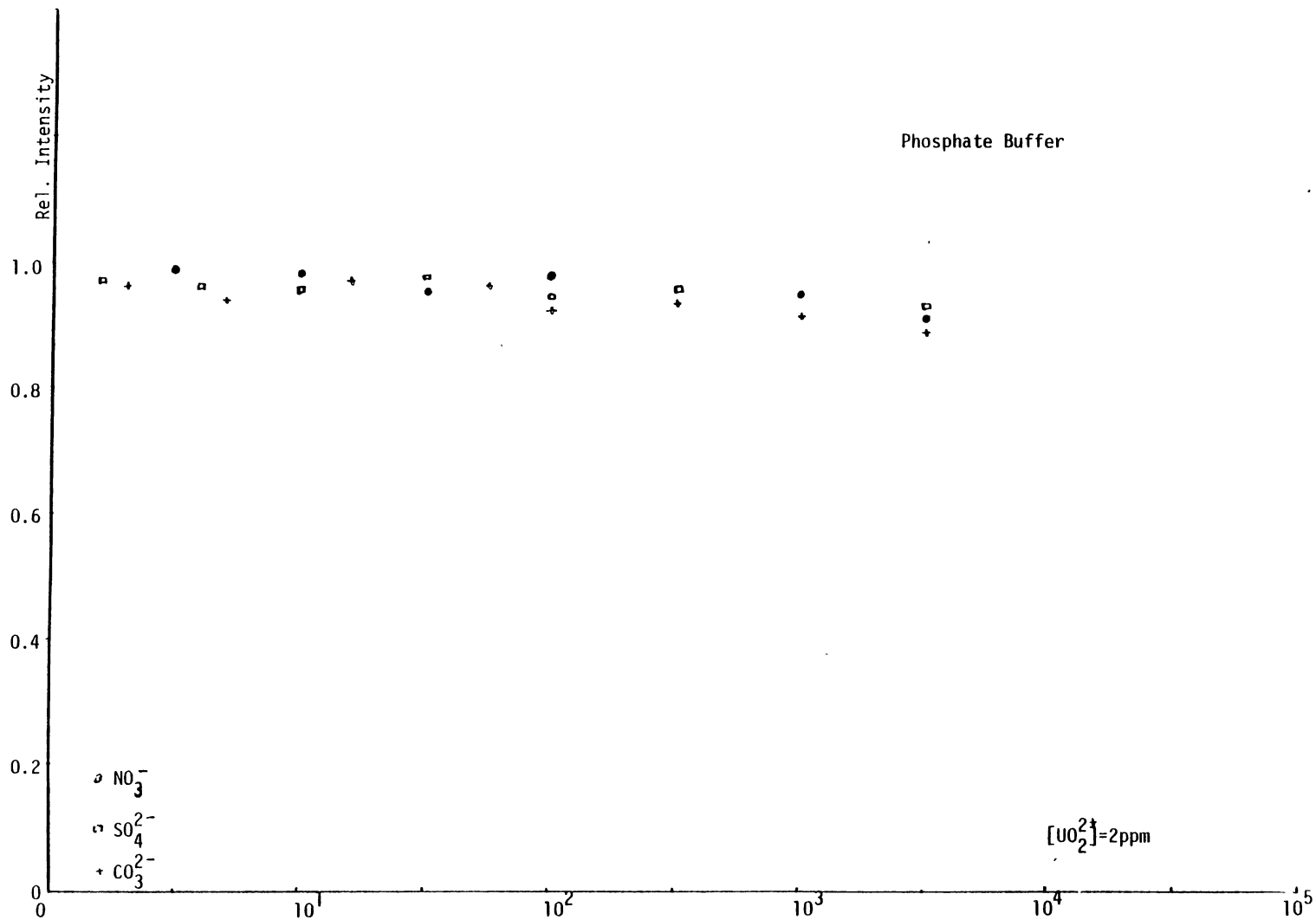


Figure 18. Fluorescence Intensity of Uranyl Ion in Phosphate Buffer As a Function of NO₃⁻, SO₄²⁻, and CO₃²⁻ Concentrations

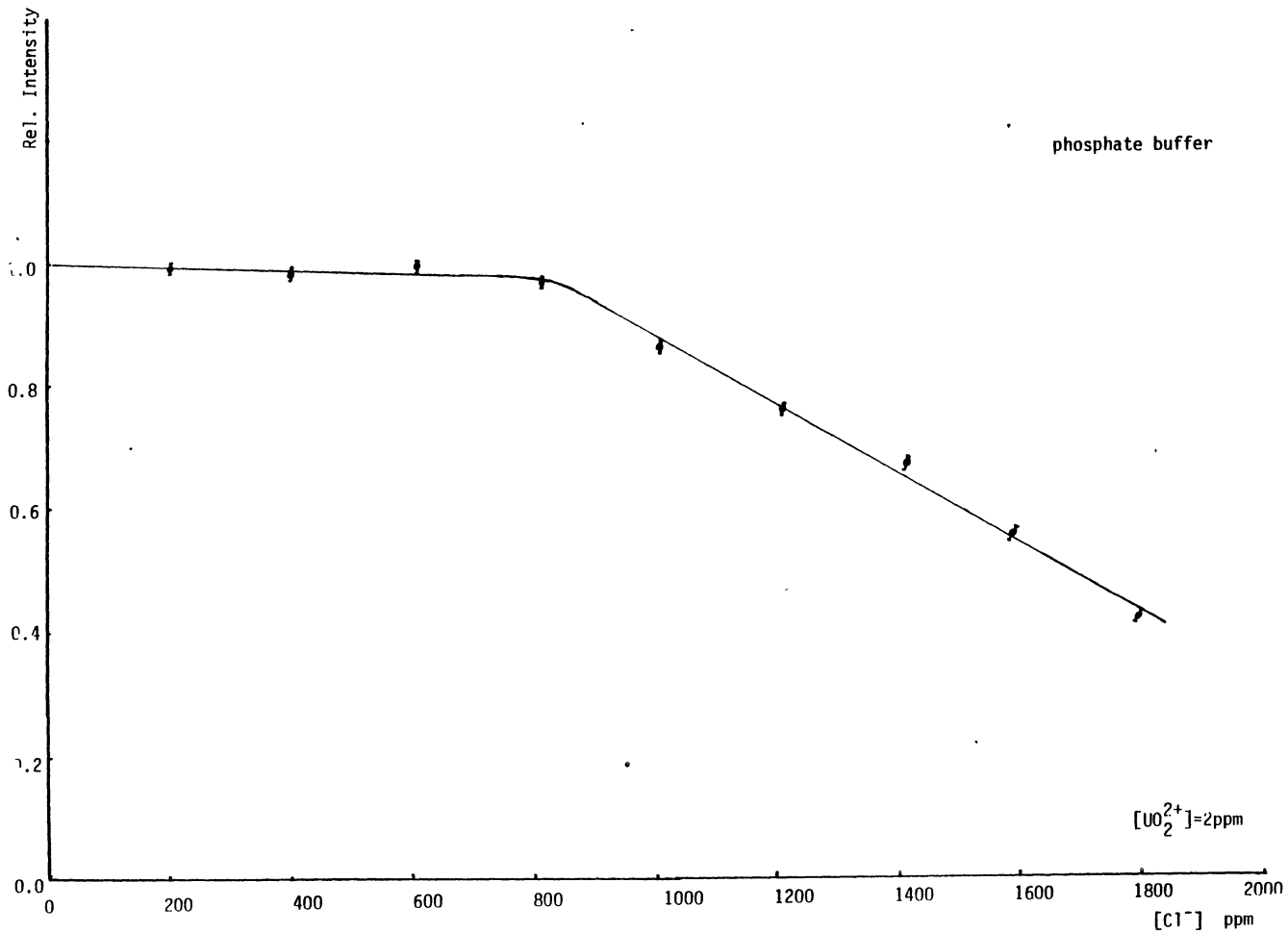


Figure 19. Fluorescence Intensity of Uranyl Ion in Phosphate Buffer As a Function of Cl⁻ Concentration

Arsenazo-III was applied to the determination of U(VI) in groundwaters and the absorbance of the uranium complex was measured.

In the procedure developed in this study, an ammonium phosphate buffer solution was used in PCR and the fluorescence of the uranyl complex measured. Since fluorescence measurement provides better sensitivity compared to absorption this method can result in lower limits of detection, which in turn reduces the sample size for the pre-concentration step.

Reagents and Materials.

HPLC grade chemicals and solvents were used throughout the procedure. HPLC grade water and monobasic ammonium phosphate were purchased from Baker Chemical Company. The post-column reagent used for the detection of U(VI) ion was ammonium phosphate buffer pH 4.3 (see section I part B) All aqueous solutions were prepared with HPLC grade water. The α -hydroxyisobutyric acid disodium salt was purchased from Sigma Chemical Company.

Apparatus.

The chromatographic system was manufactured by Micromeritics and consists of an automatic injector unit, Model 725, equipped with a standard 10- μ l loop, a ternary solvent mixer, Model 753, capable of mixing up to three solvents (isocratic), and a chromatographic pump, Model 750,

with dual reciprocating piston and hypercompensated cam operating within flow multiplexing circuitry.

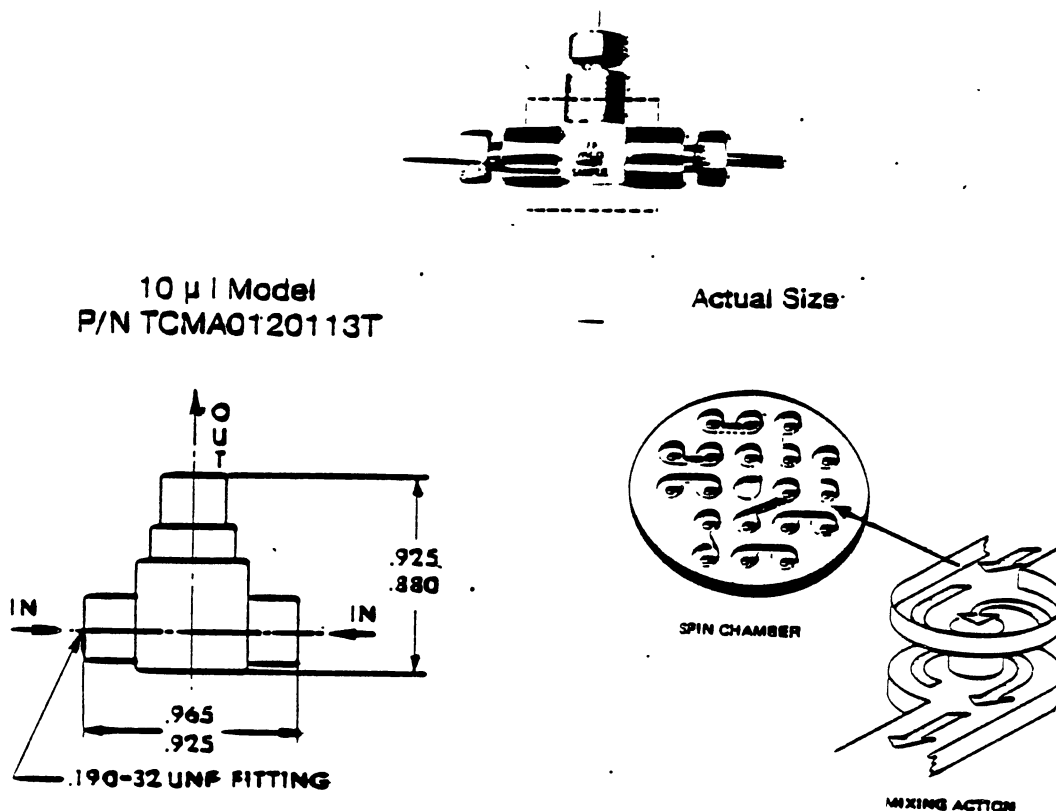


Figure 20. Schematic of Micro-Mixer manufactured by LEE company.

For PCR a Milton Roy Mini-pump and a Micro-Mixer T pipe manufactured by LEE Company were used. Schematic of the micro-mixer is shown in Figure 20.

The LEE micro-mixer operates through critically controlled series of "spin chambers" that create a succession of miniature swirling mixers. Each mixing chamber induces tangentially spinning fluids that must reduce their radius of rotation to allow passage into the next chamber, thus increasing angular velocity. This

rapidly spinning column of liquid must then reverse its own direction of rotation in order to progress to subsequent spin chambers. The result is a vigorously repeated mixing process. It has zero dead volume and an internal volume 10- μ l. A delay coil was used to allow for the completion of complex formation.

A Farrand spectrofluorometer model MK2, equipped with 150 watt DC xenon arc lamp (range of wavelength 200 to beyond 1400 nm) was used as detector

A 10- μ l fluorometric flow cell from NSG Precision Cell Inc., was used for all of the measurements.

A Radial-Pak SCX-10 μ m strong cation exchange column from Waters Division of Millipore housed in a Z-Module (Water's trade mark) was used for separation. The mean particle size for the column packing material was 10- μ m, and the column size was 8mm X 10cm.

All the data was collected by a Hewlett-Packard 3390 integrator. The components of the HPLC-PCR system are shown in Figure 21.

Chromatographic Parameters.

Aqueous solution of U(VI), typically 10- μ l, were injected on to the column (for standard solution preparation see section I part C). The elution procedure was adopted from a paper by Cassidy et al., [69]. Uranium(VI) was eluted from the cation-exchange column by 0.15 mol/liter α -hydroxyisobutyrate solution at pH = 4.5.

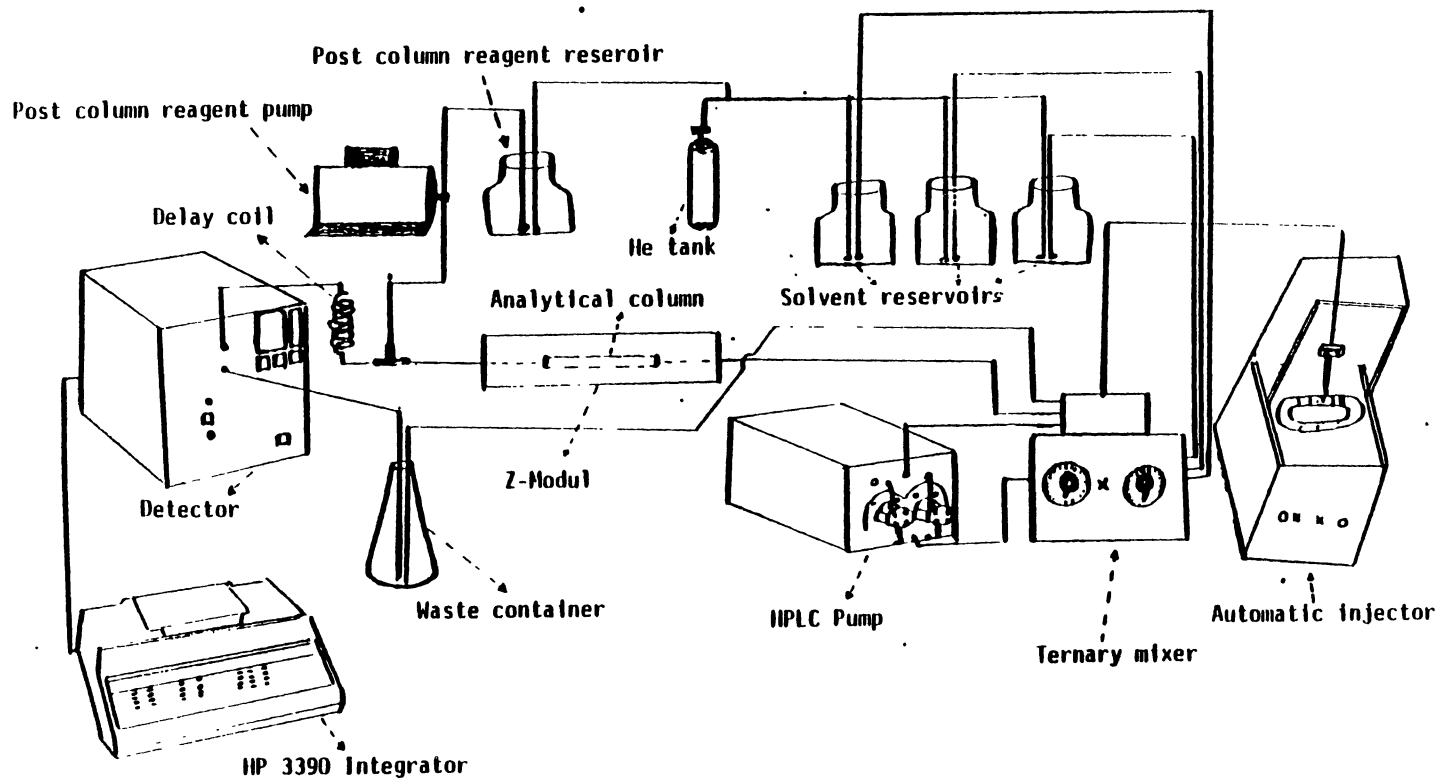


Figure 21. Post Column Reaction System Components

The U(VI) ion was detected by PCR, with ammonium phosphate solution as a fluorescence enhancing agent. Figure 22 shows the chromatogram of U(VI) ion eluted from the column in about 9 minutes.

TABLE III
CHROMATOGRAPHIC PARAMETERS FOR U(VI) SEPARATION ON
CATION-EXCHANGE COLUMN

Flow Rate (ml/min)	t_r (min)	k'	N	HETP (mm)	Efficiency (plates/meter)
2.00	8.73	2.2	1649	.061	16493
1.50	9.46	2.3	1943	.051	19432

Table III shows the effect of flow rate on the chromatographic parameters, such as k' (capacity factor), N (number of theoretical plates), HETP (height equivalent of a theoretical plate), t_r (retention time) and column efficiency (same as N but the unit is in plates/meter).

Optimization of The Reaction Coil Length.

The reaction between uranyl ions and the phosphate buffer is relatively fast to enhance the fluorescence signal of the uranium. After the uranyl ion is eluted from the column it passes through the mixer where it is mixed with the phosphate buffer and form the complex. A delay coil or commonly called reaction coil allows complete formation of

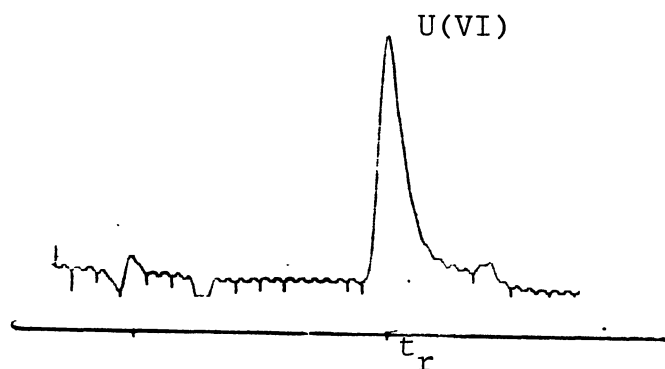


Figure 22(a). Chromatogram of Uranyl Nitrate Solution
 Column: Cation-exchange, Mobile Phase:
 x-hydroxyisobutyrate .15 mol/liter pH=4.5,
 Flow Rate 2ml/min., t_r =8.73 min., Detector
 Fluorometer, Sample Size 10-71 (200ng),
 Post-column Reagent: Ammonium Phosphate
 Buffer pH=4.30, Reaction Coil Length 1.6
 Meter, All Tubing 1/16-in. OD X .007 in. ID.

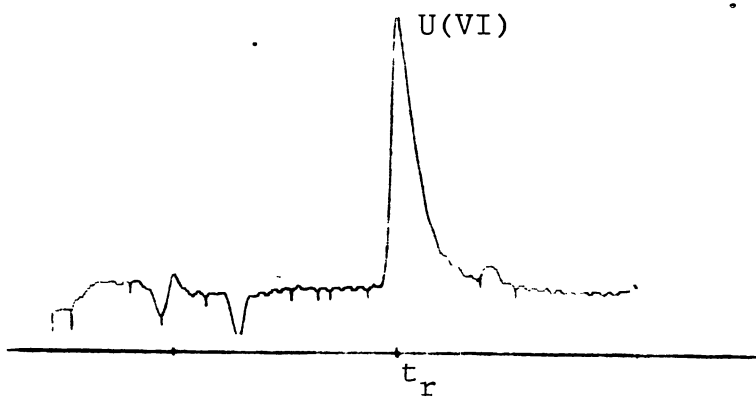


Figure 22(b). Chromatogram of Uranyl Nitrate Injected on
 Cation-exchange Column. Flow Rate
 1.5 ml/min., t_r =9.46 min., All Other
 Conditions the Same as in Figure 22(a)

the complex. The length of the reaction coil is important because too short or too long lengths cause incomplete complex formation or band broadening respectively. To find the optimum length for the reaction coil, several coil lengths were examined. Figure 23 shows the effect of coil length on the area under the peak which indicates complete complex formation.

Calibration and Detection limit.

The calibration curve was obtained by injecting varying amounts of uranyl nitrate standard solution over the range of 20 to 1600 ng of U(VI). Figure 24 shows a typical linear calibration curve up to 1600 ng obtained for the phosphate buffer detection system.

The limit of detection for the procedure was calculated according to $3 \times \text{std. dev. of intercept}$, and resulted 1 $\mu\text{g/ml}$.

Interferences.

All the cations that interfere with U(VI) measurement in section I were studied. Iron was eluted near the solvent front and up to 200 ng did not interfere with the uranium measurement.

HPLC Separation And PCR Detection Of U(VI) And U(IV) Ions In Aqueous Solutions.

There are large numbers of methods already reported for separation and determination of U(VI) [73], but no attempts

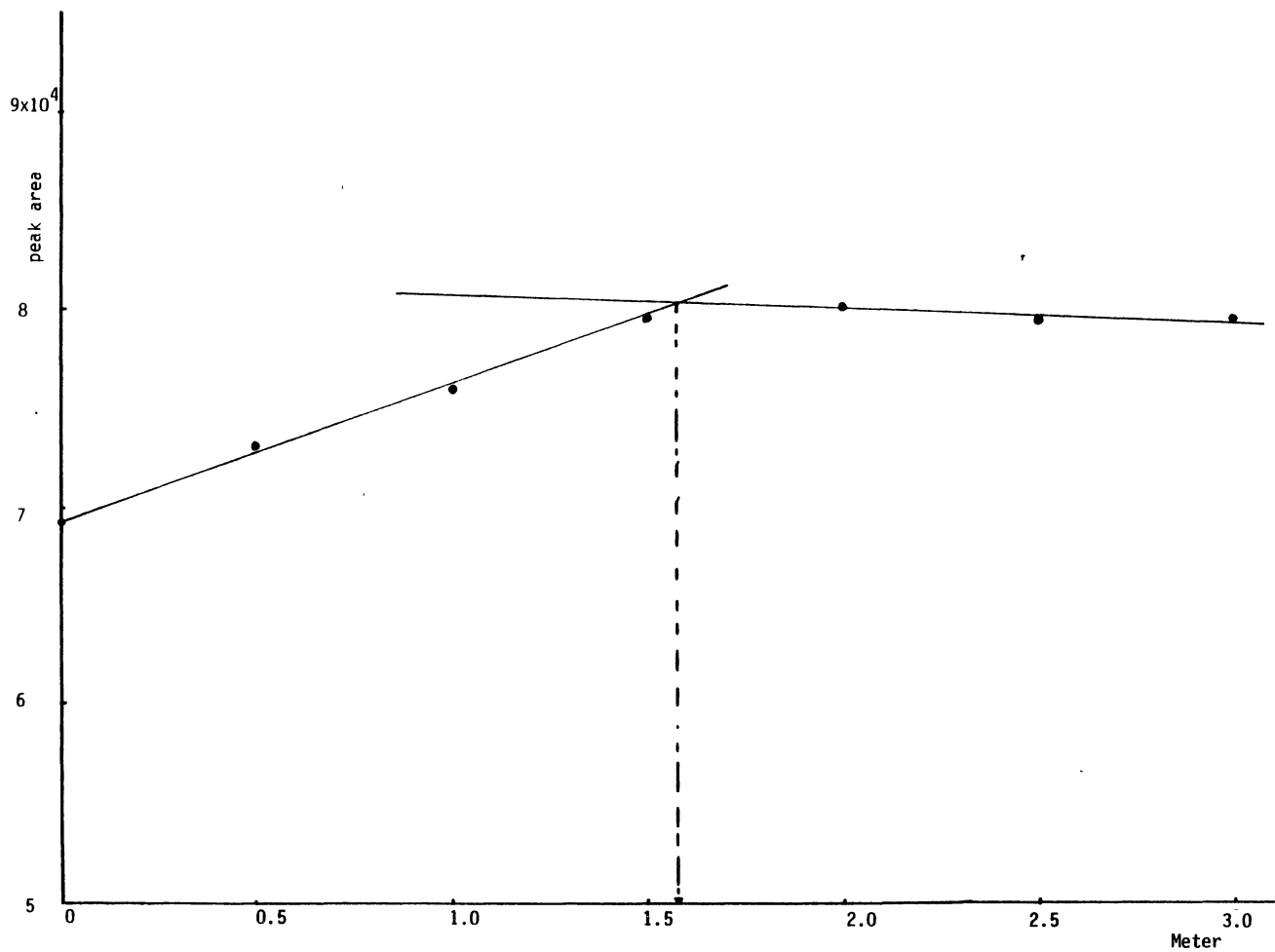


Figure 23. Optimization of Reaction Coil Length. Sample Size 800 ng.
All Other Conditions the Same as in Figure 22

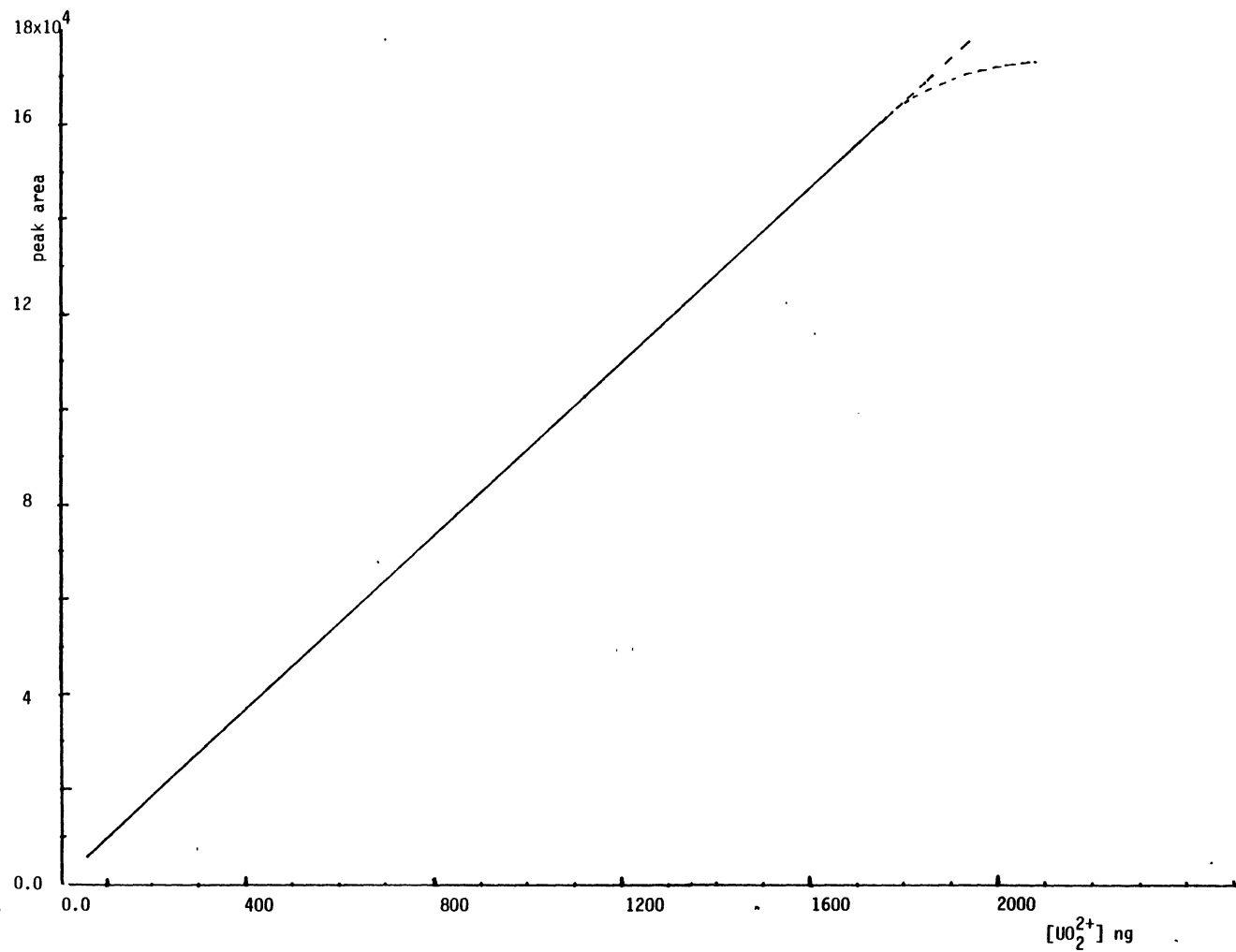


Figure 24. Calibration Curve for Uranyl Nitrate Solution. All Conditions the Same as in Figure 22

have been made on the separation and simultaneous determination of U(VI)/U(IV) ions in natural waters.

In this study a new chromatographic procedure is developed. It is based on the selective complexation of U(VI) with a complexing agent in the presence of U(IV) ions. Separation of this complex solution is performed on a reverse phase column in line with PCR using arsenazo-III.

Reagent and Materials.

All the solvents including water were HPLC grade, and purchased from Baker Chemical Company. Alkylsulfonates, (3-(2-arsenophenylazo-4,5-dihydroxy-(2-arsenophenyl)2,7-naphthalenedisulfonic acid disodium salt) known as arsenazo-III, L-phenylalanine, ethylen glycol, oligoethylene glycol, and oxalyl chloride were purchased from Sigma Chemical Company. Sodium acetate, HPLC grade, was purchased from Baker Chemical Company.

Apparatus.

The HPLC-PCR system was the same as in section II part B except for the detector. A variable UV-visible detector Model 786, from Micromeritics was used for the absorbance measurements of the uranium-arsenazo-III complex (see Figure 21).

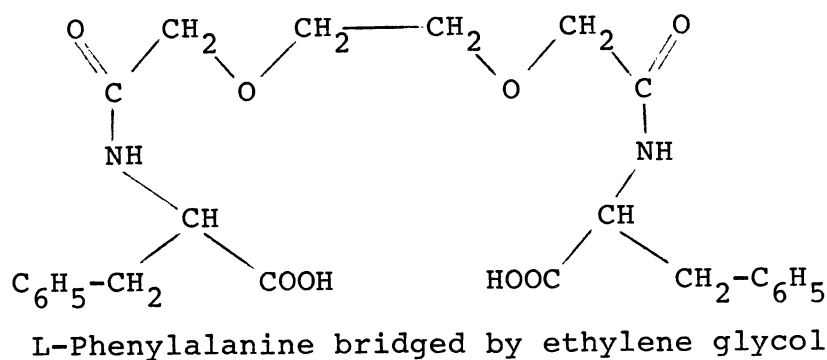
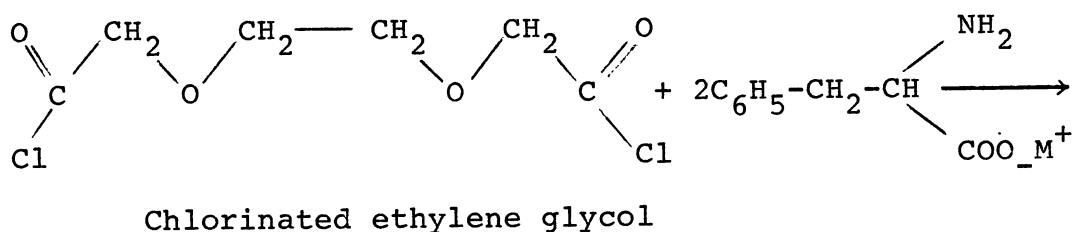
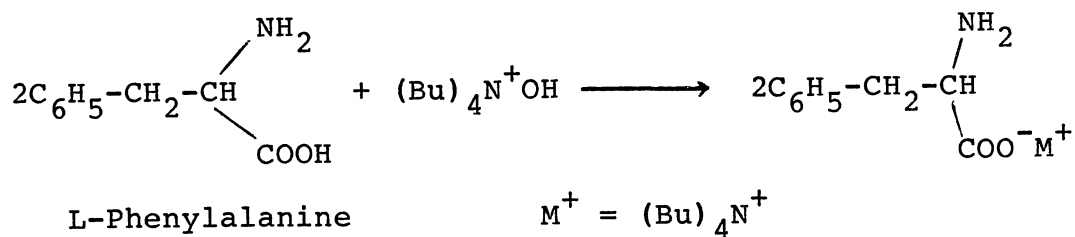
A Water's Radial-PAK C₁₈ (8mm X 10cm) with 10-um mean particle size was used for the separation.

Synthesis of ligand.

The synthesis of the acyclic ligand containing L-phenyl-alanin moities was performed according to the procedure of Marchelli et al. [74]. Two L-phenylalanine moities were linked by the ethylene oxide bridge.

Bisacid chloride. Ethylene glycol is oxidized to its corresponding diacid with nitric acid. 20 mmol of the diacid were reacted with oxalyl chloride (60 mmol) in benzene (40 ml) in the presence of a few drops of pyridine [75]. The reaction mixture was stirred for 24 hours at room temperature, then filtered and evaporated twice under vacuum in the presence of benzene and the bisacid obtained was then immediately used.

Preparation of ligand. 20 mmol of L-phenylalanine was treated with 20 mmol $(\text{Bu})_4\text{NOH}$ and dried under vacuum for one hour. The salt was then mixed with 50 ml acetonitrile under nitrogen. Bisacid chloride (10 mmol in 10 ml of solvent) was added dropwise over 1 hour. The mixture was allowed to react for 1 hour at room temperature, then it was washed four times with an acidic water and then extracted with chloroform. The organic phase was dried over Na_2SO_4 , and the solvent removed. The acid was recovered and subsequently purified by column chromatography on silica gel using chloroform as eluent.



Uranium U(VI)/U(IV) Stock Solutions.

One liter of HPLC grade water was boiled for about 10 minutes to expel CO₂ gas. After it was cooled to room temperature the water was purged with nitrogen gas to remove dissolved gases (oxygen), then helium gas was continuously bubbled into the water to keep the oxygen out. The water container was wrapped with aluminium foil (the shiny side out) to keep the light out. To this water 2.1100 g of uranyl nitrate hexahydrate and 1.5957 g of uranium (IV) chloride were added. The final concentration of U(VI) and

U(IV) was 1000 ppm in the solution. Several solutions with concentration range of 10^{-2} to 10^{-4} M were made to obtain the calibration plots.

Mobile Phase and PCR Solutions.

A 0.01 molar sodium acetate buffer solution was prepared. Alkylsulfonates were added to the acetate buffer at different concentrations. The PCR reagent was arsenazo-III with a concentration of 50 ng/ml in HCl solution of pH = 2. This reagent slowly decomposes under this condition and it must be made fresh every week.

All the solutions were purged with nitrogen gas and then with helium to remove and keep other dissolved gases and oxygen out.

Procedure.

The U(VI)-ligand complexation was performed by stirring a solution of ligand (10^{-2} M in acetonitrile) for 30 min., with an aqueous solution of uranyl nitrate and UCl_4 (10^{-4} M of each ion) at pH = 3.5. U(VI) forms a 1:1 complex with ligand at pH = 3.5 with $\log K_1 = 6.1$ [76].

An acetonitrile solution of the complex, 10- μ l, was injected on to the column. The flow rate was usually 2.0 ml/min. Different combinations of pH and eluting reagent (methanol, methanol/water, acetonitrile/water, and sodium acetate/alkylsulfonate) were used for the elution of U(VI) and U(IV) from the C_{18} column. Since the U(VI)-ligand

complex readily dissociates in HCl solution the eluted ions were detected with post column reaction with arsenazo-III solution at 655 nm.

Both U(VI) and U(IV) form complexes with arsenazo-III and produce a green solution having molar absorptivity of 53,000 and 100,000 respectively [77].

Chromatographic Parameters.

Separation and determination of U(IV)/U(VI) were performed by injecting standard solutions of the ions onto the column. Methanol, methanol/water, and acetonitrile/water were used as eluting solvents, but none of them could perform a complete separation.

An acetate buffer of 0.010 M concentration could separate the two ions at pH 4.5, but there was a problem with oxidation of U(IV) on the column. To eliminate this problem a different pH buffer was used, as can be seen in Figure 25(a-c). To improve the peak separation alkylsulfonates were added to the buffer. Figure 25(a) shows the chromatogram of U(IV)/U(VI) eluted from the C₁₈ column with 4×10^{-4} M hexanesulfonate added to the mobile phase. The flow rate was 2.0 ml/min.

Table V summarizes the chromatographic parameters calculated from the chromatograms in Figure 25.

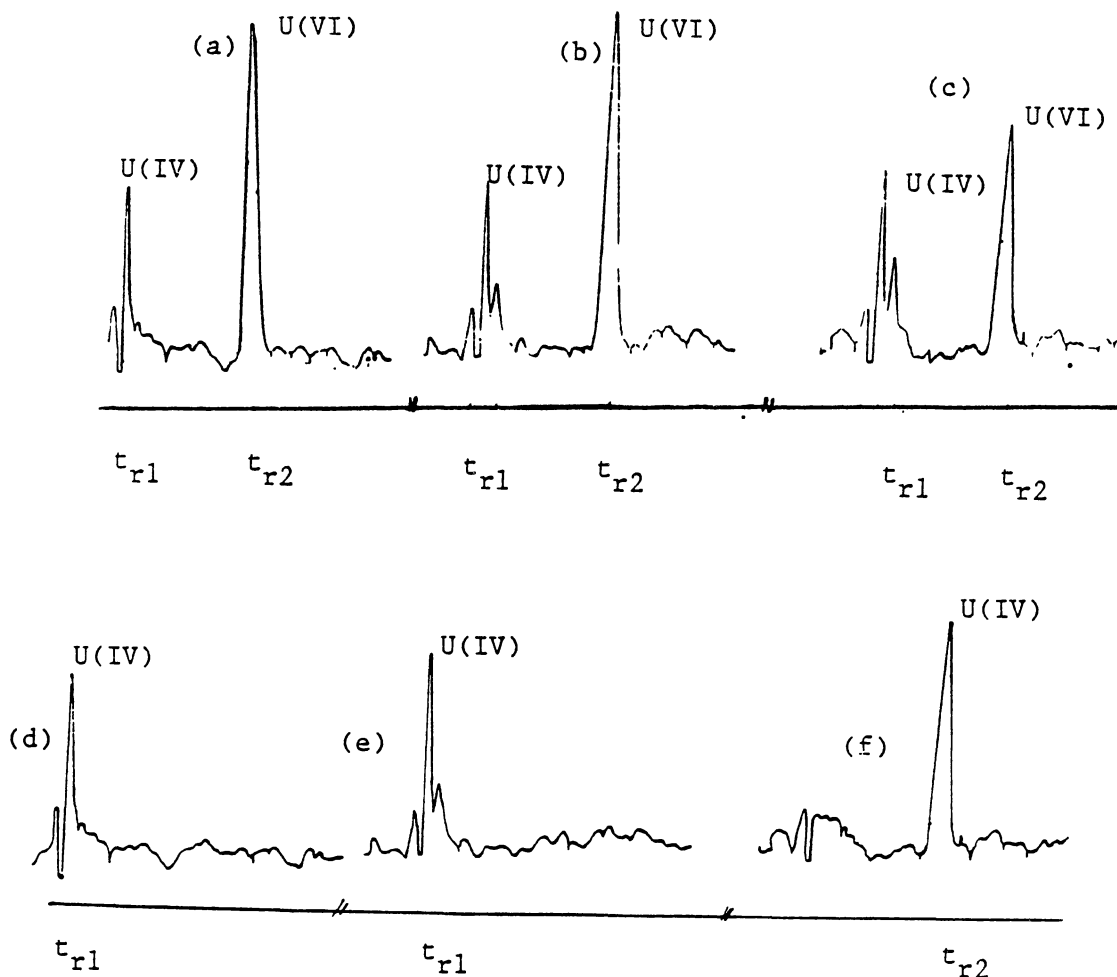


Figure 25(a). Chromatogram of U(IV)/U(VI). U(VI) Was Complexed With L-phenylalanine Moities in Acetonitrile Solution. Column C_{18} , Flow Rate 2 ml/min., $t_{r1} = 2.04$ min., $t_{r2} = 7.46$, $t_m = 1.52$ min., Mobile Phase: .01 M Sodium Acetate pH=3.5 with 4×10^{-3} M Hexanesulfonate, Sample Size 10- μ l (200 ng of Each Uranium Species), Post-Column Reagent: Arsenazo-III in HCl pH=2, Detector UV-Visible at 665 nm, Reaction Coil Length 2.1 Meter
 25(b) Mobile Phase pH=4. All Other Conditions the Same as in (a)
 25(c) Mobile Phase pH=4.5. All Other Conditions the Same as in (a)
 25(d) Chromatogram of U(IV). Conditions the Same as in (a)
 25(e) Chromatogram of U(IV). Conditions the Same as in (b)
 25(f) Chromatogram of U(VI). Conditions the Same as in (a)

TABLE IV
 CHROMATOGRAPHIC PARAMETERS FOR U(IV)/U(VI) SEPARATION
 ON C₁₈ COLUMN. CONDITIONS OF THE RUN
 IS GIVEN IN FIGURE 25

U(IV)		U(VI)	
Flow rate(ml/min.)	2.00	t _m (min.)	1.52
t _{r1} (min.)	2.04	t _{r2} (min.)	7.46
k' ₁	0.71	k' ₂	3.91
N	678	HETP	.032
Efficiency(plate/meter)	6780	R _s	3.25
HETP	1.5	N	3105
(selectivity)	5.3	Efficiency	31050

Effect of pH And Ionic Strength of The Buffer Solution
 On U(IV)/U(VI) Separation.

The effect of pH of the acetate buffer on the separation of uranium (VI) and U(IV) was studied. Figure 25 a, b, and c, shows that at pH = 3.5 the side peak at t_r = 2.63 min. is eliminated and only peak due to the solvent front and two peaks due to U(IV) and U(VI) were recorded.

The dependence of the capacity ratio of the U(IV) and U(VI) on the acetate buffer concentration was studied at pH=3.5. Figure 26 shows the plot of k' vs ionic strength of the acetate solution.

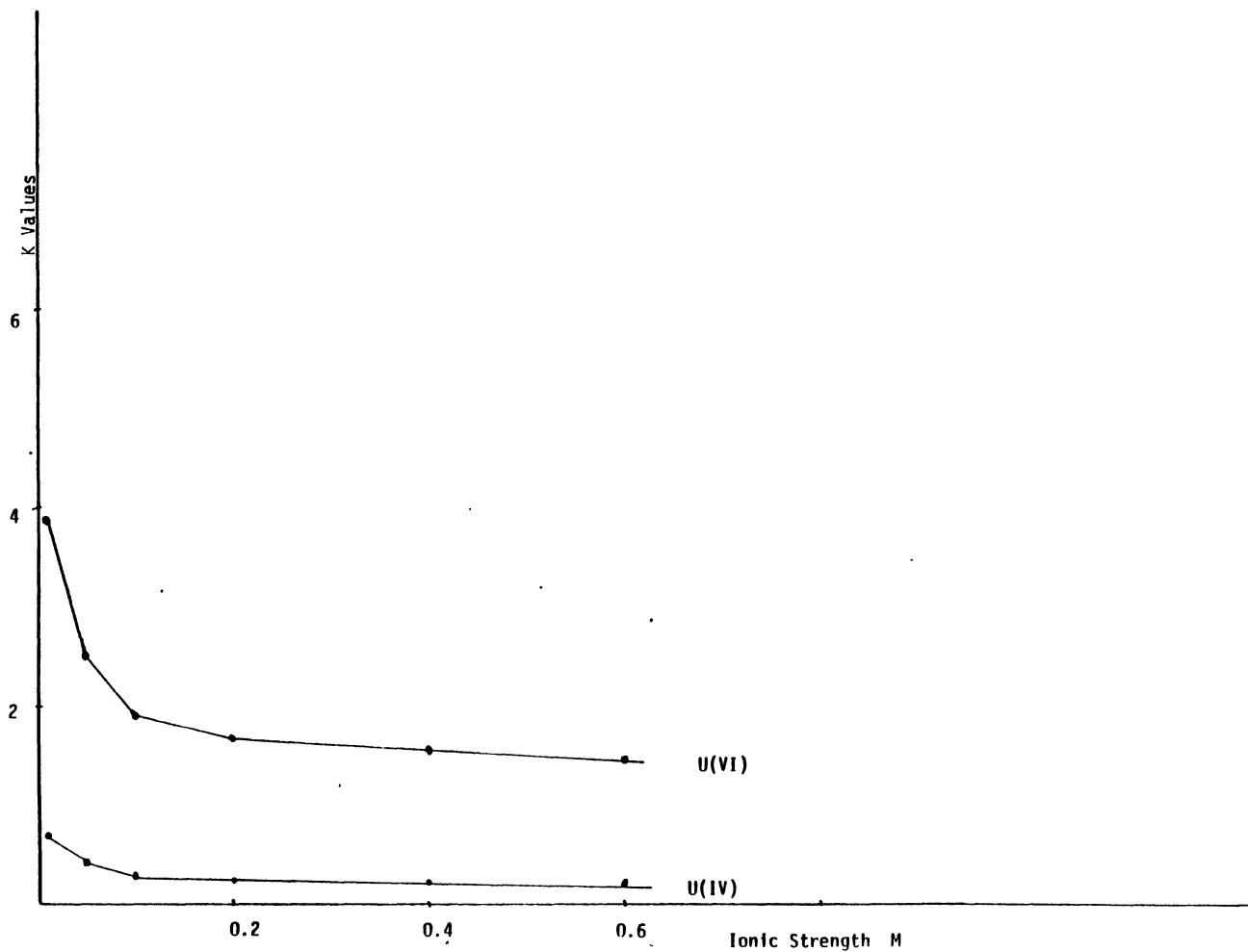


Figure 26. Dependence of the Capacity Factor of U(VI) and U(IV) on the Acetate Buffer Concentration. No Ion-pairing Reagent in the Mobile Phase. All Other Conditions the Same as in Figure 25(a)

Effect of Alkylsulfonates Chain Length on k' Values.

The dependence of the capacity ratio of the U(IV) and U(VI) on the side chain of the alkylsulfonates was studied. The purpose was to select an alkylsulfonate which could produce the best possible separation parameters for the uranium species. Figure 27 shows the plot of k' vs n at various concentrations of alkylsulfonates.

After the above test, hexanesulfonate was used as the ion-pairing compound throughout the study. Hexanesulfonate at various concentrations in the mobile phase was studied to find the best concentration for ion-pairing in this procedure. Figure 28 shows the dependence of k' value on the concentration of hexanesulfonate.

The reaction coil was optimized according to the procedure in section II part D. The length of the reaction coil obtained from the data was 2.1 meter.

Calibration Curve and Detection Limit.

The calibration curve was obtained by injecting varying amounts of U(VI)-ligand and U(IV) solution over the range of 25 to 1500 ng of both U(VI) and U(IV). The calibration curve was linear over the range of study and tended to level off at the higher concentration. Figures 29 and 30 shows the calibration curve for U(VI) and U(IV) respectively. To evaluate the procedure, standard sample solutions were injected on the column and the integrator was programmed to calculate and report the area under the peaks and the amount

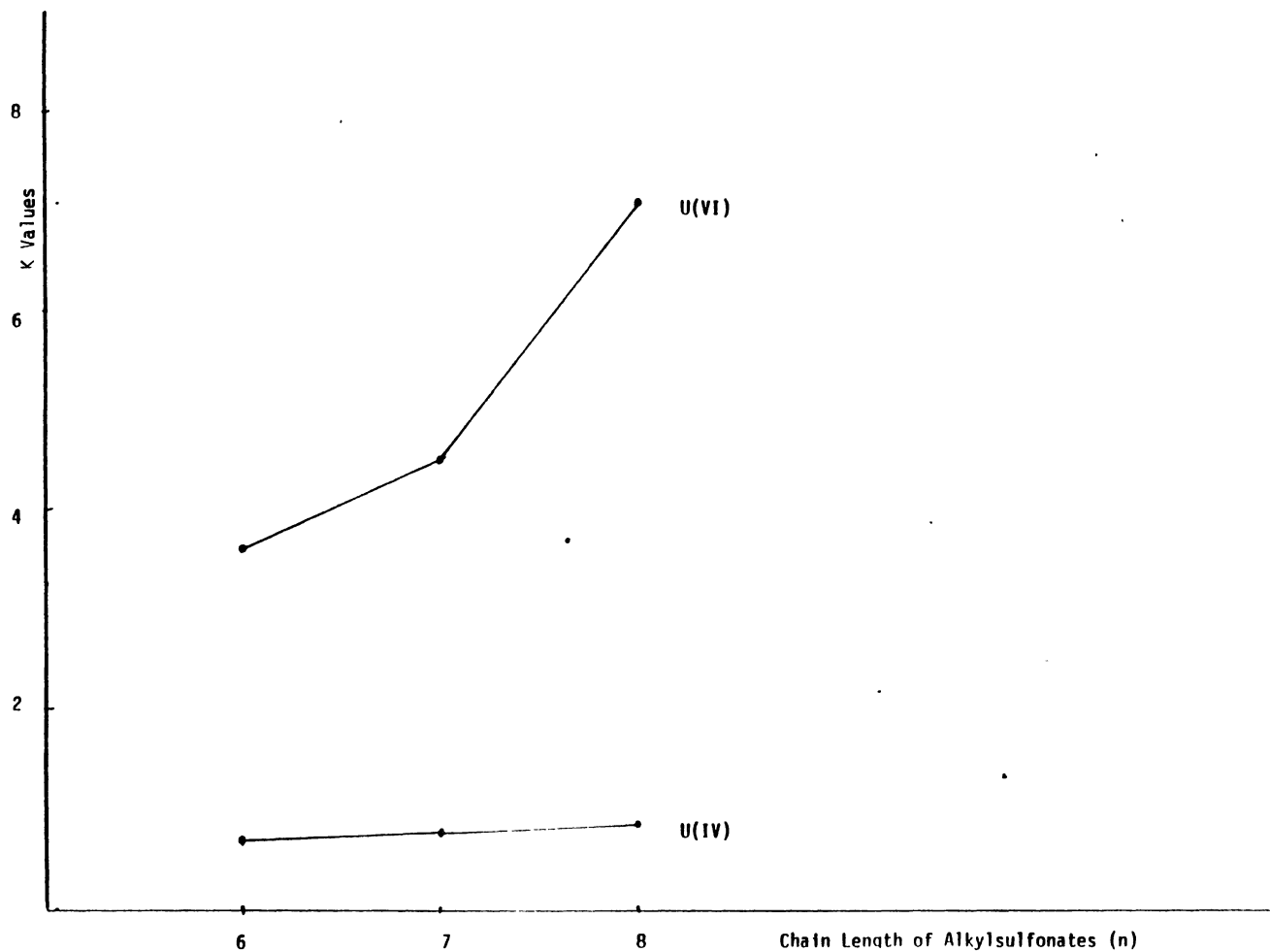


Figure 27. Dependence of the Capacity Factor of U(VI)/U(IV) on the Side-chain Length of the Alkylsulfonates. Mobile Phase 0.1 M Acetate Buffer. All Other Conditions the Same as in Figure 25(A)

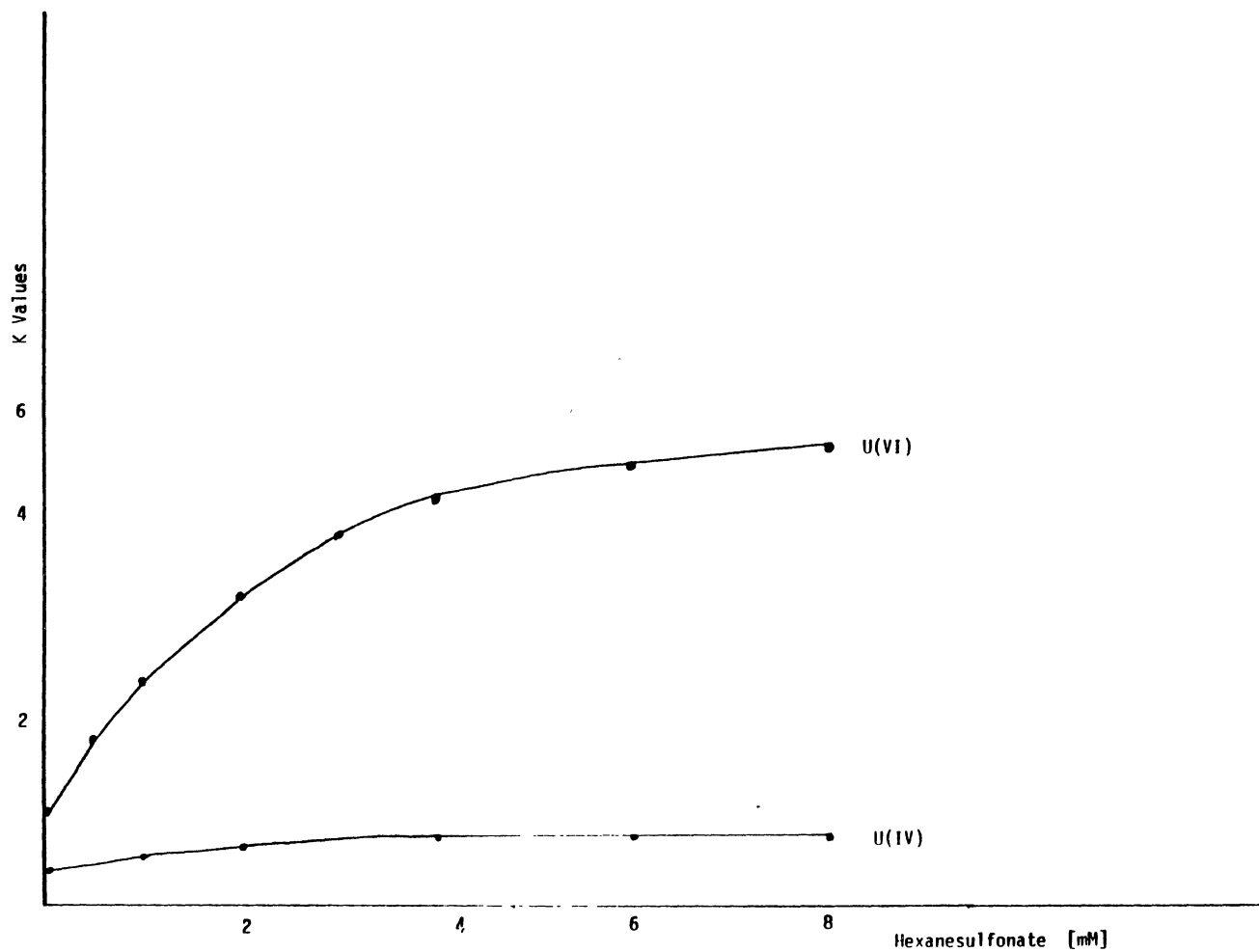


Figure 28. Dependence of the Capacity Factor of U(IV)/U(VI) on the Concentration of Hexanesulfonate. Mobile Phase Contain .1 M Acetate Buffer. All Other Conditions the Same as in Figure 25(a)

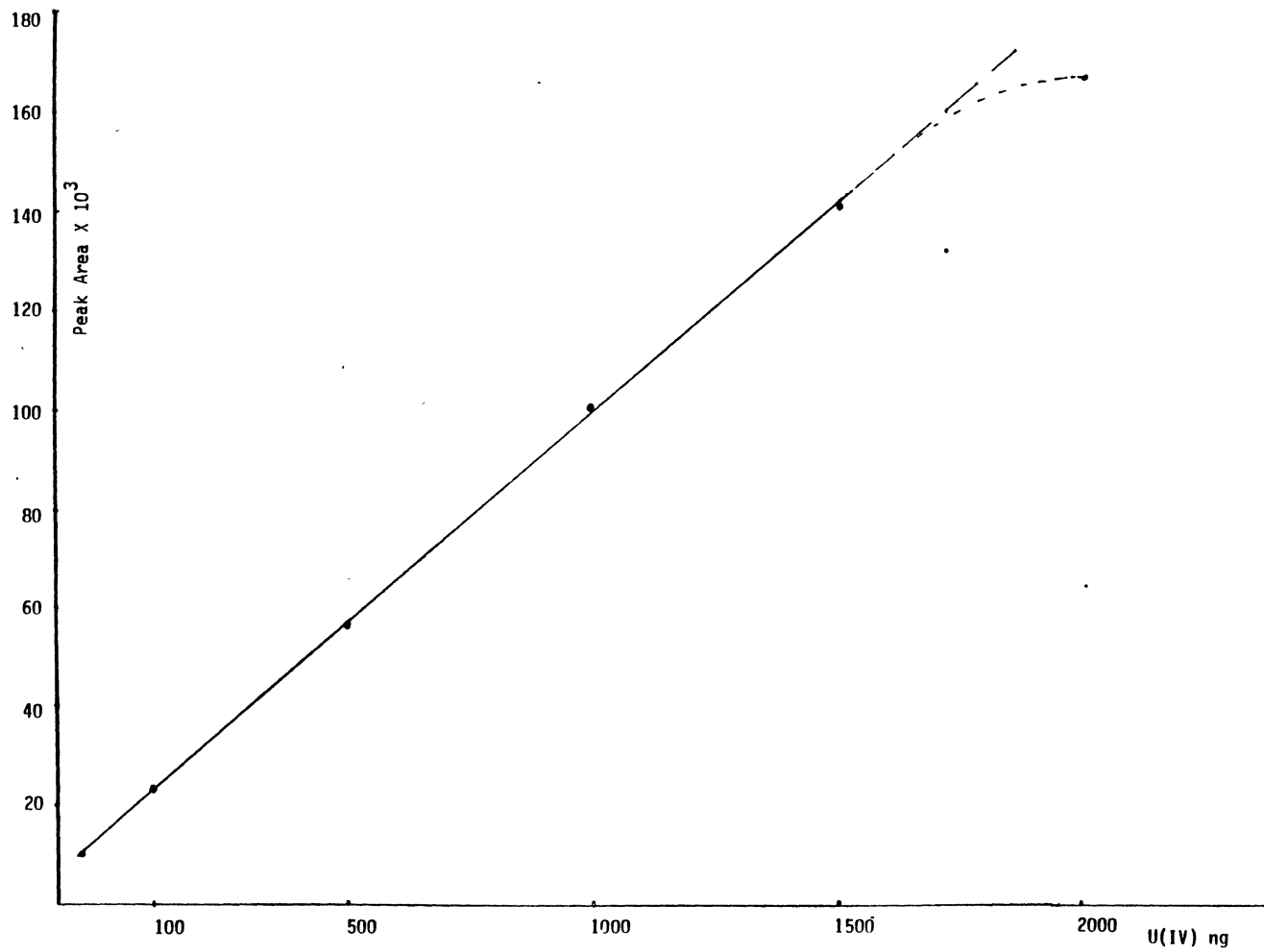


Figure 29. Calibration Curve for U(IV) on C₁₈ Column. All Other Conditions the Same as in Figure 25(d)

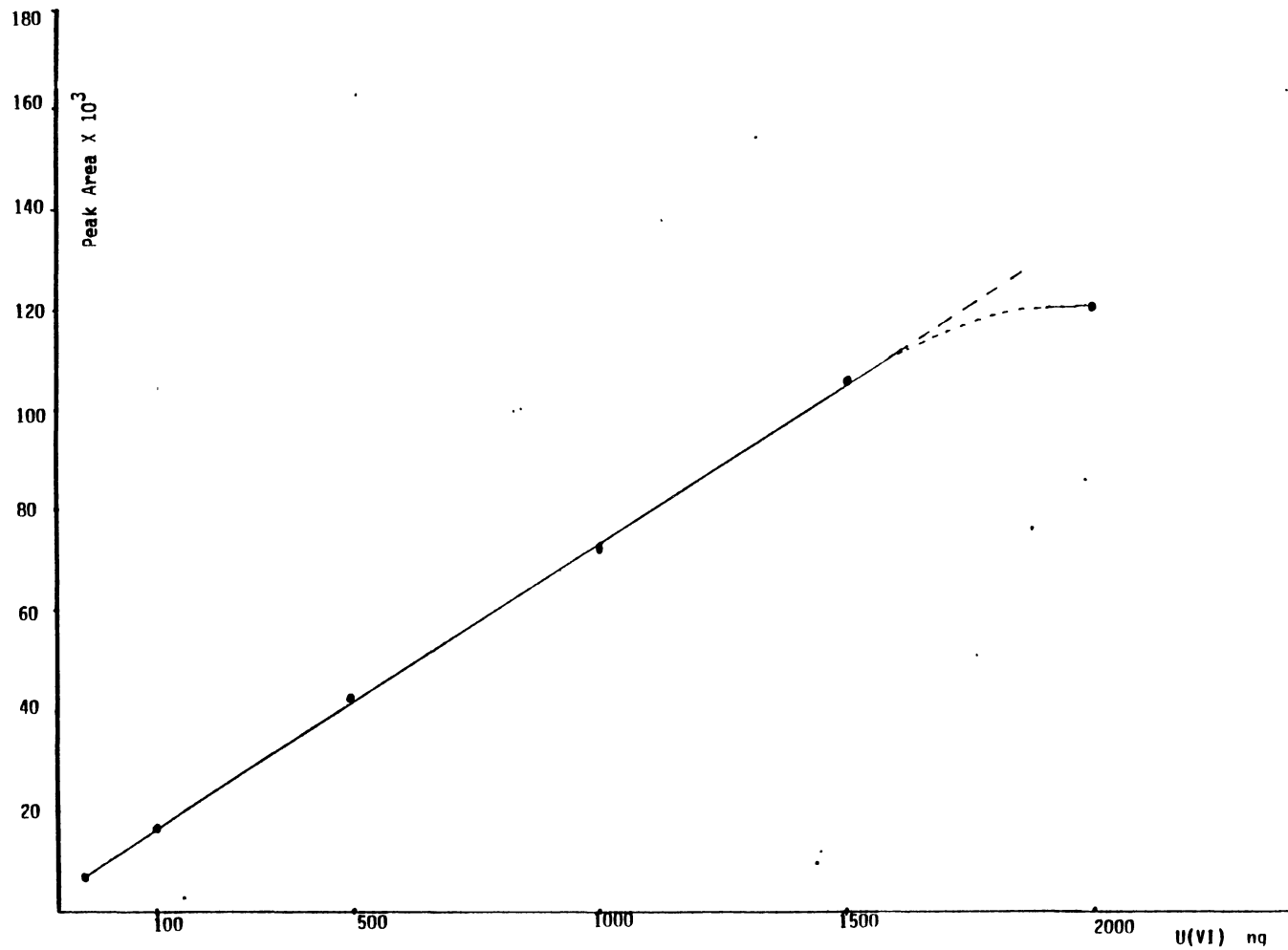


Figure 30. Calibration Curve for U(VI) on a C₁₈ Column. All the Conditions the Same as in Figure 25(f)

of the ions. Then a series of samples were injected and the concentrations were compared to the standard. The standard deviation from the mean was less than 0.5% in most cases.

The detection limit of each ion was calculated by the method of three times standard deviation of intercept. The values for the limit of detection of the procedure were 0.7 $\mu\text{g/ml}$ for U(IV) and 1.2 $\mu\text{g/ml}$ for U(VI).

Interferences.

The major interfering ion in this procedure was iron which eluted near the solvent front and complexed with arsenazo-III. To eliminate this problem ascorbic acid was added to the solution containing iron and iron was kept the in Fe(II) state so as not to react with the detection reagent under the experimental conditions used.

CHAPTER IV

RESULTS AND DISCUSSION

Direct Fluorometric Determination Of U(VI) In Aqueous Solutions.

Regression analysis was applied to the calibration data to produce the plot in Figure 11. The correlation coefficient of the line was 0.9986, $m = 3.6286$, $b = 415.71$, and the standard deviation of the intercept was 141.02.

The detection limit calculated by the method of three times standard deviation of intercept was 2 ppb. The signal-to-noise ratio method resulted in a lower value of 1 ppb for the detection limit (Figure 12). The method of three times standard deviation of intercept is commonly used to report the detection limit of the procedure, since it is a better estimate of the sensitivity for the measurement. The signal-to-noise ratio gives the limit of detection for the detector and not for the procedure [78].

The complexation of U(VI) with phosphate solution is fast and the fluorescence signal due to the complex is stable for more than 4 hours. At $\text{pH} = 4.36$ and excess of HPO_4^{2-} , the $\text{UO}_2(\text{HPO}_4)_2^{2-}$ complex is the only uranyl ion specie in the solution [79].

In this procedure the 30 ml of buffer solution marked the upper limit of complexing solution needed to reach maximum fluorescence intensity due to the uranyl phosphate complex (Figure 13).

In order to specify the uranium concentration region in which the standard addition method is valid, a linear response range has been determined. Variation of fluorescence intensity vs uranium concentration over ranges of 0.5-50 ppm and 50-400 ppb were noted. Figure 14 shows marked deviation from linearity in the 0.5-50 ppm range. The calibration curve was linear when the uranium concentration was less than 2 ppm. Values greater than 2 ppm showed deviation from linearity, indicating that 2 ppm is an upper limit to linear response. Solutions containing uranium in the upper range require dilution into the linear range, which also helps to reduce the effect of interfering ions

Figures 15, 16, 17 and 18 show the relative fluorescence intensity as a function of main cation concentrations expected in surface or ground water. As can be seen in Figure 15, concentrations of Na^+ , K^+ , or Mg^{2+} up to 10,000 ppm do not interfere for U(VI) measurement in this procedure.

Iron and manganese, often cited as examples of transition metals that quench uranium fluorescence, can occur at significant concentrations in the natural environment. The quenching effect of these metals depends,

for a given concentration of the interfering species, on the photochemistry of the particular uranyl complex involved. Their presence provides alternative pathways for deactivation of the energy absorbed by the uranyl complex at the expense of uranyl fluorescence. The most critical elements are Mn, Fe, and Ca. Figure 16 shows that Mn at <8 ppm (which is greater than the usual amount of Mn^{2+} in natural water) do not interfere. Figure 17 and 18 shows that Fe at <4 ppm and Ca at <5 ppm do not interfere with U(VI) measurement in this procedure.

In the analysis of 100 river basin water samples, Reiders et al., [80], reported maximum values of 0.71 and 0.029 ppm for Fe and Mn respectively; while many values reported were less than 0.001 ppm Fe and 0.001 ppm Mn. Ground waters will carry higher levels of dissolved-solids. Gabelman [81] reported, a range of 0.02-1.3 ppm Fe and 0.20 ppm Mn for spring and well water. According to Garrett and Lynch [82] there is a positive correlation among uranium, Fe, and Mn; in which higher interferences were accompanied by higher uranium values. If this is true, an appropriate dilution of the sample can minimize any interferences in this procedure.

If a simple dilution of the sample solution can not reduce the effect of the interfering ions down to about 20% reduction of sensitivity of fluorescence signal (20% reduction in fluorescence signal would be an acceptable value in geochemical exploration), then an alternative would

be an HPLC separation of uranium from interfering ions. This topic will be discussed in the following sections.

The dependence of the fluorescence signal on the concentrations of NO_3^- , $\text{SO}_4^{=}$, and $\text{CO}_3^{=}$ is shown in Figure 18. It is evident that these anions have no effect on fluorescence intensity of the uranyl ion in this procedure. The only anion that interferes with the measurement is Cl^- ion. At a concentration >1000 ppm, Cl^- ions do interfere with the U(VI) measurement, noting this concentration is well above the amount of Cl^- ion in surface and ground waters.

Most of the methods for uranium determination in aqueous solutions need a pre-concentration or even a complete separation step before the uranium can be measured. The separation lowers the detection limit because of the enrichment factor and eliminates interfering ions; however, any separation step is time consuming and expensive. The fluorometric determination of uranium developed in this study provides a rapid and sensitive method for U(VI) measurement in the presence of interfering ions. The procedure can be applied without any separation or enrichment step and can be recommended for the measurement of low U(VI) concentrations when the number of samples are high.

HPLC Separation Post-Column Fluorometric Determination Of U(VI) In Aqueous Solutions.

Uranium (VI) was eluted from the cation-exchange column with 0.15 mol/liter solution of α -hydroxyisobutyrate. The retention time of U(VI) was about 9.46 min. The detection was done by post-column reaction using a pH 4.3 ammonium phosphate buffer as a complexing agent. A 1.6 meter reaction coil was used to allow complete complex formation. Figure 23 shows the relationship between the area under the peak and the length of the reaction coil. An increase in the length of the reaction coil (over 1.6 meter) seemed to have no effect on the area under the peak, but caused further bandbroadening.

A linear calibration curve was obtained for the phosphate buffer detection system over the range 50 to 2000 ng of U(VI). The relative standard deviation for multiple injection of about 800 ng of U(VI) was <1%. The upper limit for The amount of U(VI) seems to be about 2000 ng, at this point the calibration curve starts to deviate from linearity. The correlation coefficient of the calibration line was 0.9984 with the slope of 7.264, $b = 6.528$ and standard deviation of the intercept was 2.417. From the regression analysis data the detection limit was calculated to be about 1 $\mu\text{g/ml}$. This is the detection limit of the procedure not for the detector which would be lower than 1 $\mu\text{g/ml}$.

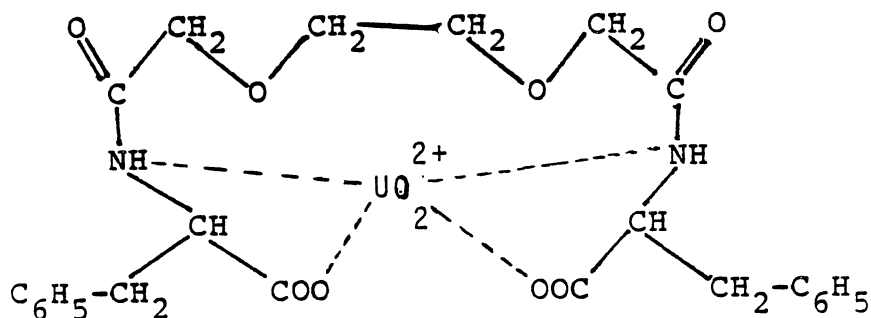
In the HPLC separation of U(VI) on a cation-exchange column most of the interfering cations will elute at or near the solvent front which eliminates their interfering effect.

This study has shown that the bonded-phase cation exchanger with a post-column reaction using phosphate buffer solution offers a relatively rapid, selective, and sensitive method for separation and determination of U(VI) in the samples containing relatively high amounts of interfering ions.

HPLC Separation and PCR Detection Of U(IV) and U(VI) Ions In Aqueous Solutions.

The uranyl ion in aqueous solution is complexed with the L-phenylalanine ligand (see below) at various pH values and different ligand/U(VI) ratios. The degree of complexation is influenced by the pH of the solution. At pH of about 3, maximum complexation occurs when the ligand is present as a dianion, giving a 1:1 complex of U(VI) in presence of excess ligand. The high selectivity of the ligands for U(VI) was ascertained by competition experiments with other cations. Among all the metals, only Cu^{2+} may complex with the ligand in very small quantities. Uranium(IV) did not complex with the ligand at any metal-to-ligand ratio tested [74].

According to T. Lodi [76] the amide- and carboxylic groups are involved in complexation to U(VI). Their results are based on a C^{13} -NMR study of the metal-ligand complex in methanol.



L-Phenylalanine bridged by ethylene glycol
Complexed with UO_2^{2+}

Arsenazo-III was used as the post column reagent for determination of U(VI)/U(IV) species. Arsenazo-III solution was prepared in 0.25 mol/liter HCl at pH = 2 (the reagent slowly decomposes and therefore must be made fresh each time).

The U(VI)-complex totally dissociates in acidic solutions of pH about 2 and form a complex with arsenazo-III which absorb light at 665 nm. Uranium(IV) also complexes with arsenazo-III and absorbs light at 665 nm.

Experimental results suggested that 2.1 meters was the optimum length for the reaction coil. This provided enough time for the reaction to reach equilibrium.

To perform the separation of U(VI)/U(IV) species, 10- μ l of the treated solution was injected on the column. Optimum separation was obtained with 0.01 M acetate buffer of pH = 3.5 containing 4×10^{-3} M hexanesulfonate. Under these conditions, U(IV) was not retained on the column and was

eluted near the solvent front, while the U(VI)-complex was eluted later in the mobile phase. If hexanesulfonate is not used in the mobile phase, poor resolution is observed.

Increasing the retention of the solutes by manipulating the pH of the mobile phase proved unsuccessful. Consequently, efforts were made to find an additional modifier which will be able to influence the retention of the U(VI)-ligand complex. Thus alkylsulfonate as ion-pairing solution was added to the mobile phase. The selection of hexanesulfonate as ion-pairing reagent was based on the data plotted in Figure 27 which shows that hexanesulfonate gives a k' value of about 3.6. Other alkylsulfonates with higher chain length gave higher k' values. Plotted results in Figure 28 suggests that 4 mM concentration of hexanesulfonate is a reasonable value for the concentration in mobile phase.

The behaviour of the U(VI)-complex in the presence of the ion-pairing reagent suggests that the complex should be a charge-transfer type and the overall charge on the molecule is positive.

During the course of experimentation it became apparent that ionic strength is a very important factor affecting the retention time, resolution and the reproducibility of the system. Experiments were performed over a wide range of concentrations, and therefore the influence of ionic strength on k' value was studied. To ascertain the contribution of ionic strength to the capacity factor, the

effect of changing the concentration of the acetate buffer in the mobile phase containing only the buffer was studied. The buffer concentration of 0.01 M was obtained by studying the Figure 26. At lower concentrations of the buffer a better k' value was obtained.

Although the behavior of the k' value is typical and in general well understood, several points should be made. The decrease is most noticeable at low concentrations of the acetate where the drop in the capacity factor is quite rapid (see Figure 26). At higher concentrations the change in k' value is much more moderate. For that reasons the sulfonate studies described above were carried out at a buffer concentration of 0.1 M. In this manner, ionic strength effects due to the sulfonate concentration changes are kept to a minimum. The effect of the ionic strength, as shown in Figure 26, is similar for both uranium species. This fact is of theoretical importance when one is attempting to isolate the various interactions between the additives and the solutes.

When the uranium species were separated on the column with the buffer and ion pairing compound at a pH of 4.5 a side peak next to the U(IV) was observed. The peak was suspected to result from the oxidation of U(IV) on the column. When the pH of the buffer was lowered below 4.5 the side peak began disappearing. At pH 3.5 the peak totally disappear. The area under the U(IV) peak tends to increase as the pH was decreased, while the side peak was

disappearing. These observations suggest that the side peak was possibly due to the oxidation of U(IV) on the column.

To evaluate the analytical potentiality of this procedure in uranium determination and to state the concentration range in which it could be applied, the dependence of the peak area on the quantity of U(VI) and U(IV) injected was obtained individually and simultaneously. The dependence of the peak area on the quantity of U(VI) was linear in the range of 20-1500 ng of U(VI) injected. A calibration plot was constructed (Figure 29). The regression analysis of the data resulted in $r = 0.9989$, $m = 8.652$, $b = 12.110$, and the standard deviation of the intercept was 4.383. The detection limit for the U(VI) with this procedure was about 1.2 $\mu\text{g/ml}$. In the case of U(IV) the dependence was linear in the range of study and the statistical values were $r = 0.9982$, $m = 6.486$, $b = 8.023$, and the standard deviation of the intercept was 2.825. The detection limit of the procedure for U(IV) was calculated to be about 0.7 $\mu\text{g/ml}$. The upper concentration limit for U(VI)/U(IV) detection with this procedure seems to be about 1700 ng, (Figures 29-30)

These results have not been confirmed on a wide range of real samples, but indicate that the proposed method could be effective and highly selective in the separation and determination of uranium species in aqueous samples at ppb concentration levels.

CHAPTER V

SUMMARY

Three methods have been evaluated and proposed for separation and determination of uranium ions in this study.

- (1). Direct fluorometric determination of U(VI).
- (2). HPLC-PCR separation and detection of U(VI) on cation-exchange column.
- (3). Reversed-phase HPLC-PCR separation and detection of U(IV)/U(VI) on C₁₈ Column.

The procedure applied the fluorometric method for direct detection of U(VI) in aqueous solutions. Ammonium phosphate buffer of pH = 4.36 was added to a suitable aliquot of uranium sample. At pH 4.36 phosphate complexes the uranyl ion and enhances its fluorescence signal. The complex was then excited at 285 nm and the fluorescence signal was measured at 525 nm. The limit of detection for the procedure was about 2 ppb. The upper concentration limit of 2 ppm was observed.

The effect of interfering anions and cations commonly present in natural water were studied. Cations such as Na⁺, K⁺, and Mg²⁺ up to 10,000 ppm do not interfere. Iron at <4 ppm, Mn at <8 ppm and Ca at <5 ppm do not interfere, while higher concentrations do interfere with the measurement. The

effect of NO_3^- , $\text{SO}_4^{=}$ and $\text{CO}_3^{=}$ on fluorescence signal showed no interfering due to these anions. But Cl^- at concentration higher than 1000 ppm start to interfere with the measurment. Overall, this procedure is a direct, rapid, sensitive and simple method for U(VI) determination in aqueous samples.

The second part of the study used high-performance liquid chromatography, post-column reaction, and a fluorometer to separate and detect the uranyl ion. Ten ul of a suitable aliquot of uranium sample was injected on the cation-exchange column. Uranium (VI) was eluted from the column with α -hydroxyisobutyrate at pH = 4.5. The eluted ion was mixed with ammonium phosphate buffer in a PCR system and the fluorescence intensity of the complex was measured by a fluorometer. The limit of detection for the procedure was about 1 $\mu\text{g}/\text{ml}$ of U(VI). Iron which is the major interfering ion, was eluted from the column near the solvent front and no interfering effect up to 200 ng of Fe in the sample was observed. This procedure provide a rapid, selective and sensitive method for separation and determination of U(VI) ions.

The last part of the study, developed a method for separation and determination of U(IV)/U(VI) species in aqueous solutions.

Reversed-phase liquid chromatography with post-column reaction and a UV-visible detector was used to separate the uranium species.

Uranium(VI) was complexed with L-phenylalanine moiety. Then a solution containing U(VI)-complex and U(IV) was injected on a C₁₈ column and eluted with 0.01 M sodium acetate buffer solution. In order to improve the conditions of the separation, hexanesulfonate as an ion-pairing compound was added to the mobile phase. Uranium(IV) and U(VI) were separated with retention times of 2.04 min. and 7.46 min. respectively. Following the post-column reaction of uranium ions with arsenazo-III, the absorbance of the complexes were measured at 665 nm. The influence of ionic strength, chain length and concentration of alkylsulfonate were investigated. These parameters are shown to provide powerful tools to manipulate selectivity. The effect of acetate buffer concentration on the capacity factor was studied. The limits of detection for the procedure were 0.7 µg/ml and 1.2 µg/ml for U(IV) and U(VI) respectively.

The results of the study indicate that the proposed procedure could be very effective and highly selective for the separation and determination of uranium species at the ppb concentration level.

BIBLIOGRAPHY

1. Klaproth, M. H., Chem. Ann., Bd. 2, 387 (1789).
2. Klaproth, M. H., Chem. Ann., Bd. 1, 292 (1090).
3. Palei, P. N., in Analytical Chemistry of Uranium, Ann arbor-Humphrey Science, London, 1970, P.13.
4. Sen Sarma, R. N., Mallik, A. K., Anal. Chim. Acta, 12, 329 (1955).
5. Reinhardt, K. H., Muller, H. J., Z. Anal. Chem. , 292, 359-361 (1978).
6. Sillen, L.G., Martell, A. E., in Stability Constants of Metal-Ion Complexes, The Chemical Society (London). special publication No. 17, 1964, P. 49-450.
7. Martell, A. E., Smith, R. M., in Critical Stability Constants vol. 1, Plenum Press, New York, 1975, P. 25-390.
8. Katz, J., Seaborg, G., in The Chemistry of Actinide Elements, John Wiley, New York, 1957, P. 184.
9. Ibid, vol. 3, 1977, P. 2-265.
10. Bachelet. M., Claude, R., Lederer, M. M., Compt. rend., 240,419 (1955).
- 11 Rao, G., Somideramma, G., Z. anal. Chem., 157, 27 (1957).
12. Sacconi, L., Giannoni, G., J Chem. Soc., P. 2368 (1954).
13. Firurz, J. S., Bradford, S. K., Anal. Chem., 30, 1021 (1958).
14. Baes, C. F., Mesmer, R. E., in The Hydrolysis of Cations, Wiley Interscience, New York, 1976, P. 489.
15. Seaborg, G. T., Katz, J., in The Actinide Elements, McGraw-Hill, New York, 1954, P. 137-180.

16. Litzke, M. H., Stoughton, R. W., J. Phys. Chem., 64, 816-820 (1960).
17. Hearne, J., White, A., J. Chem. Soc., P. 2168 (1957).
18. Maekoya, C., Takata, Y., Bull. Soc. Sea Water Sci. (Japan), 33, 337-342 (1980).
19. Takata, T., Mizuniwa, F., Maekoya, C., Anal. Chem., 51, 2337-2339 (1979).
20. Masushima, Y., Yonezawa, K., Mizuniva, F., Takata, Y., Thermal and Nuclear Power, (tokyo), 29, 671-677 (1978).
21. Cassidy, R. M., Elchuk, S., J. Chromatogr. Sci., 18, 217-223 (1980)
22. Lundfren, D. P., Loeb, N. P., Anal. Chem. 33: 66-370 (1961).
23. Takata, Y., Arikawa, Y., Buneski Kagaku 24: 762-767 (1975).
24. Fritz, J. S., Story, J. N., Anal. Chem. 46: 825-829 (1974).
25. Small, H., Stevens, T. S., Bauman, W. C., Anal. Chem. 47: 1801-1809 (1975).
26. Pollard, F. H., Nickless, G. Rofers, D. E., Rothwell, M. T., J. Chromatogr. 17: 157-167 (1965).
27. Spackman, D. H. Stein, W. H., Moore, S., Anal. Chem. 30: 1190 (1958).
28. Deelder, R. S., Kroll, M. G. F., Beeren, A. J., Van Den Berg, M., J. Chromatogr. 149: 669-682 (1978).
29. Hirai, Y., Yoza, N., Ohashi, S., Anal. Chim. Acta 115: 269-277 (1980).
30. Hirai, Y., Yoza, N., Ohashi, S., J. Chromatogr. 206: 501-509 (1981)
31. Yoza, N., Ito, K., Hirai, Y., Ohashi, S., J. Chromatogr. 196: 471-480 (1980).
32. Sickafoose, J. P., Ph.D. Thesis, Iowa State University, IS-T-498 (1971).

33. Kawazu K., Fritz, J. S., J. Chromatogr. &&: 397-405 (1973).
34. Kawazu, K., Shibata, M., Kakiyama, H., J. Chromatogr. 115: 543-542 (1975).
35. Matsui, H., Anal. Chim. Acta 66: 143-146 (1973),
36. Elchuk, S. Cassidy, R. M., Anal. Chem. 51: 1434-1438 (1979).
37. Story, J. N., Fritz, J. S., Talanta 21: 894-896 (1974).
38. Schmidt, G. J., Scott, R. P. W., Analyst 109: 997-1002 (1984).
39. Katz, E. D., Scott, R. P., J. Chromatogr. 268: 169 (1983).
40. Riviello, J., Fitchett, A., Johnson, E., Dionex Technical Note (1983).
41. Riviello, J., Pohl, C. A., Dionex Technical Note 1983 and 1984 Pittsburgh Conference.
42. Cassidy, R. M., Elchuk, S., J. Chromatogr. Sci. 18: 217-223 (1980).
43. Dasgupta, P. K., Anal. Chem. 56: 96-103 (1984).
44. Hirose, A., Iwasaki, I., Iwata, I., Ueda, K., Ishii, D., J. HRC & CC 4: 530-531 (1981).
45. Marsh, K. C., Sternson, L. A, Repta, A. J., Anal. Chem. 56: 491-497 (1984).
46. Engelhardt, H., Neue, U. D., Chromatographia, 15: 403-408 (1982).
47. Shih, Y. T., Carr, P. W., Anal. Chim. Acta 159: 211-228 (1984).
48. Uiklein M., Schwab, E., Chromatographia, 15: 140 (1982).
49. Hobbs, P. J., Jones. P., Ebdon, L., Anal. Proc. 20: 613-616 (1983).
50. Lawrence. J. F., Brinkman, U. A. T., Frei, R. W., J. Chromatogr. 171: 73-80 (1979).
51. Apffel, J. A., Brinkman, U. A. T., Frei, R. W., Chromatographia 18: 5-10 (1984).

52. Cassidy, R. M., Elchuk, S., J. Liq. Chromatogr. 4: 379-398 (1981).
53. Kucera, P., Umugat, H., J. Chromatogr. 255: 563-579 (1983).
54. Dasgupta, P. K., Bligh, R. Q., Mercurio, M. A., Anal. Chem. 57: 484-489 (1985).
55. Jones, P., Hobbs, P. J., Ebdon, L., Anal. Chim. Acta 149: 39-46 (1983).
56. Takata, Y., Arikawa, Y., Japan Analyst. 22: 312-318 (1973)
57. Takata, Y., Arikawa, Y., Muto, G., Bunseki Kagaku. 26: 407-411 (1977).
58. Dorey, R. C, Frank, J., Seiler Research Laboratory, Report FJSRL-TR-81-0005 (1981).
59. Hartkopf, A , Delumyea, R., Anal. Lett. 7: 79-88 (1974).
60. Beckett, J. R., Nelson, D. A., Anal. Chem. 53: 911-914 (1981)
61. Fleming, H. D., Ide, R. G., Anal. Chim. Acta. 83: 67 (1976).
62. Shaikh, A. U., Tallman, D. E., Anal. Chim. Acta. 98: 251 (1978)
63. Nakahara, T., Anal. Chim. 131: 73 (1981).
64. DeOliveria, E., McLaren, J. W., Berman, S. S., Anal. Chem. 55: 2047 (1983).
65. Kawazu, K., J. Chromatogr. 137: 381-396 (1977).
66. Bushee, D. S., Krull, I.S., Demko, P. R., Smith, S. B. Jr., J. Liq. Chromatogr. 7: 861-876 (1984).
67. Brazell, R. S., Homberg, R. W., Moneyhun, J. H., J. Chromatogr. 290: 163-172 (1984).
68. Knight, A. R., Smith, S. D., Anal. Chim., Acta, 146: 42-51 (1982)
69. Cassidy, R. M., Elchuck, S., Intern. J. Envir. Anal. Chem. 10: 287-294 (1981).

70. Dianelson, A., Raennhalm, B., Ingman, F., Talanta, 20(2): 185-190 (1973).
71. Snell, F.D., Photometric and Fluorometric Methods of Analysis, Part 11, John Wiley and Sons, P. 1373 (1978).
72. Sverdrup et al., The Ocean, P. 150 (1942).
73. Zhi-Lin, W., Xia-Nian, C., Fu-Xin, L., Anal. Chim. Acta, 160: 295-299 (1984).
74. Marchelli, R., Dradi, E., Dossena, A., Casnati, G., Tetrahedron, 38 (14): 2061-2067 (1982).
75. Dietrick, B., Lelz, J. M., Sauvage, J. P., Blanzat, J., Tetrahedron, 29: 1629-1635 (1973).
76. Lodi, T., Marchelli, R., Dossena, A., Dradi, E., Casnati, G., Tetrahedron, 38 (18): 2055-2060 (1982).
77. Sanvin, S. B., Talanta, 8: 673-685 (1961).
78. Ruthley, L., Anal Chem., 52, 2242-6 (1980)
79. Langmuir, D., U.S. Department of Energy, GJO-1659-3, P. 5-25 (1977)
80. Reeder, S. W., Hilton, B., Levinson, A. A., Geochem. Cosm. Acta., 36: 825-86 (1972)
81. Gabelman, J. W., IAMPL-391/21, Proc. Panel. Uranium Expl. Geol., Viena (1970)
82. Garret, R. G. J., Lynch, J., IAEA-SM-208130, Proc. Symp. Expl. For Uranium Ore Deposit, Viena (1976)

2
VITA

Abdol Reza Karimi

Candidate for the Degree of

Doctor of Philosophy

Thesis: HPLC SEPARATION POST-COLUMN REACTION, UV-VISIBLE AND FLUORESCENCE DETECTION OF TRACE UO_2^{2+}/U^{4+} SPECIES IN AQUEOUS SOLUTIONS

Major Field: Chemistry

Biographical:

Personal Data: Born in Tehran, Iran, February, 20, 1948, the son of Alahgholi and Zahra Karimi. Married to Fereshteh Keyhany on may 25, 1978.

Education: Graduate from Jaffari High School, Tehran, Iran, in May, 1967; received bachelor of science Degree in Chemistry from Pars College in May, 1971; received Master of Science in Biochemistry from Eastern New Mexico University in may, 1976; received Master of Science in Petroleum Engineering from The University of Tulsa in December 1978; completed requirements for the Doctor of Philosophy degree at Oklahoma State University in August, 1986.

Professional Experience: Plant Supervisor, Parchin Chemical Company, Tehran, Iran, August, 1971, to December, 1973; Teaching Assistant, Department of Chemistry, Eastern New Mexico University, January, 1974, to December, 1975; Research Assistant, Department of Petroleum Engineering, The University of Tulsa, August, 1976, to December, 1978; Teaching Assistant, Department of Chemistry, Oklahoma State University, January, 1979, to December, 1984; Manager of the Nutrition Laboratories, Department of Animal Science, Oklahoma State University, February, 1985, to present.